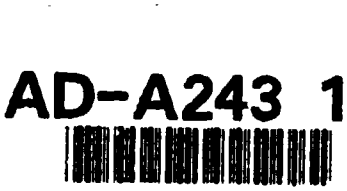

(2)

NAVAL POSTGRADUATE SCHOOL
Monterey, California

THESIS

A WING ROCK MODEL FOR THE F-14A AIRCRAFT

by

Steven Roland Wright

June 1992

Thesis Advisor: Louis V. Schmidt

Unclassified

SECURITY CLASSIFICATION OF THIS PAGE

REPORT DOCUMENTATION PAGE

Form Approved OMB No. 0704-0188

1a. REPORT SECURITY CLASSIFICATION: UNCLASSIFIED	1b. RESTRICTIVE MARKINGS
2a. SECURITY CLASSIFICATION AUTHORITY	3. DISTRIBUTION/AVAILABILITY OF REPORT: Approved for public release; distribution is unlimited.
2b. DECLASSIFICATION/DOWNGRADING SCHEDULE	
4. PERFORMING ORGANIZATION REPORT NUMBER(S)	5. MONITORING ORGANIZATION REPORT NUMBER(S)
6a. NAME OF PERFORMING ORGANIZATION: Naval Postgraduate School; 6b. OFFICE SYMBOL (If applicable): 31	7a. NAME OF MONITORING ORGANIZATION: Naval Postgraduate School
6c. ADDRESS (City, State, and ZIP Code): Monterey, California 93943-5000	7b. ADDRESS (City, State, and ZIP Code): Monterey, California 93943-5000
8a. NAME OF FUNDING/SPONSORING ORGANIZATION; 8b. OFFICE SYMBOL (If applicable)	9. PROCUREMENT INSTRUMENT IDENTIFICATION NUMBER
8c. ADDRESS (City, State, and ZIP Code)	10. SOURCE OF FUNDING NUMBERS: PROGRAM ELEMENT NO; PROJECT NO; TASK NO; WORK UNIT ACCESSION NO.

11. TITLE (Include Security Classification)

A WING ROCK MODEL FOR THE F-14A AIRCRAFT

12. PERSONAL AUTHOR(S) Wright, Steven R.

13a. TYPE OF REPORT	13b. TIME COVERED	14. DATE OF REPORT (Year, Month, Day)	15. PAGE COUNT
Engineer's Thesis	FROM _____ TO _____	June 1992	86

16. SUPPLEMENTARY NOTATION
The views expressed in this thesis are those of the author and do not reflect the official policy or position of the Department of Defense or the U. S. Government.

17 COSATI CODES			18. SUBJECT TERMS (Continue on reverse if necessary and identify by block number)
FIELD	GROUP	SUB-GROUP	Wing Rock, F-14A, Nonlinear Flight Mechancis, Aircraft Stability.

19. ABSTRACT (Continue on reverse if necessary and identify by block number)

An investigation of inertial coupling and its contribution to wing rock in the F-14A aircraft has been conducted. Wind tunnel data was used to obtain the stability parameters for angles of attack from zero to 25 degrees, after which linear and nonlinear analyses of the equations of motion were completed. The linearized analysis of the uncoupled longitudinal and lateral-directional equations was included to provide a baseline for comparison with the fully coupled, nonlinear equations. In both cases, the equations of motion were solved numerically and time history traces produced to illustrate aircraft response. Results indicate that a stable short period mode can feed damping energy into an unstable dutch roll mode via the coupling of the equations to produce a stable limit cycle very similar to those experienced in the aircraft. Numerous suggestions for follow on research are presented.

20. DISTRIBUTION/AVAILABILITY OF ABSTRACT: ☒ UNCLASSIFIED/UNLIMITED ☐ SAME AS RPT ☐ DTIC USERS	21. ABSTRACT SECURITY CLASSIFICATION: Unclassified
22a. NAME OF RESPONSIBLE INDIVIDUAL: Schmidt, Louis V.	22b. TELEPHONE (Include Area Code): (408) 646-2972; 22c. OFFICE SYMBOL: AA/Sc

DD Form 1473, JUN 86 *Previous editions are obsolete.* S/N 0102-LF-014-6603

SECURITY CLASSIFICATION OF THIS PAGE Unclassified

Approved for public release; distribution is unlimited.

A WING ROCK MODEL FOR THE F-14A AIRCRAFT

by

Steven Roland Wright
Lieutenant, United States Navy
B.S., United States Naval Academy, 1984
M.S., Naval Postgraduate School, 1990

Submitted in partial fulfillment of the requirements
for the degree of

AERONAUTICAL AND ASTRONAUTICAL ENGINEER

from the

NAVAL POSTGRADUATE SCHOOL
June 1992

Author: Steven Roland Wright
Steven Roland Wright

Approved by: Louis V. Schmidt
Louis V. Schmidt, Thesis Advisor

Richard M. Howard
Richard M. Howard, Second Reader

E. R. Wood
Dr. E. Robert Wood, Chairman, Department of Aeronautics and Astronautics

Richard S. Elster
Richard S. Elster, Dean of Instruction

ABSTRACT

An investigation of inertial coupling and its contribution to wing rock in the F-14A aircraft has been conducted. Wind tunnel data was used to obtain the stability parameters for angles of attack from zero to 25 degrees, after which linear and nonlinear analyses of the equations of motion were completed. The linearized analysis of the uncoupled longitudinal and lateral-directional equations was included to provide a baseline for comparison with the fully coupled, nonlinear equations. In both cases, the equations of motion were solved numerically and time history traces produced to illustrate aircraft response. Results indicate that a stable short period mode can feed damping energy into an unstable dutch roll mode via the coupling of the equations to produce a stable limit cycle very similar to those experienced in the aircraft. Numerous suggestions for follow on research are presented.

TABLE OF CONTENTS

LIST OF FIGURES

TABLE OF SYMBOLS AND ABBREVIATIONS

Aerodynamic Parameters

C_D	Drag coefficient, dimensionless
C_{D0}	Drag coefficient at zero lift
C_L	Lift coefficient, dimensionless
C_{L0}	Lift coefficient at AOA = 0
$C_{L_{thrust}}$	Contribution of thrust to lift coefficient
C_{m0}	Pitching moment coefficient at AOA = 0
$C_{m_{cg}}$	Pitching moment coefficient about aircraft c.g.
$C_{m_{thrust}}$	Contribution of thrust to pitching moment coefficient

Geometric and Inertial Parameters

b	Wingspan, ft.
c	Mean aerodynamic chord, ft.
I_{xx}	Moment of inertia about x axis, slug ft^2
I_{yy}	Moment of inertia about y axis, slug ft^2
I_{zz}	Moment of inertia about z axis, slug ft^2
I_{xz}	Product of inertia , slug ft^2
m	Aircraft mass, slugs

Stability Analysis Parameters

C_l	Rolling moment coefficient, dimensionless
C_m	Pitching moment coefficient, dimensionless
C_n	Yawing moment coefficient, dimensionless

C_y	Side force coefficient, dimensionless
C_z	Vertical force coefficient, dimensionless
$L_{( )}$	Rolling moment dimensional derivative
$M_{( )}$	Pitching moment dimensional derivative
$N_{( )}$	Yawing moment dimensional derivative
$Y_{( )}$	Side force dimensional derivative
$Z_{( )}$	Vertical force dimensional derivative
$( )_{\dot{\alpha}}$	Variation with dimensionless AOA rate, $\dot{\alpha}c/2U$
$( )_{\alpha}$	Variation with angle of attack
$( )_{\beta}$	Variation with sideslip angle
$( )_{\delta s}$	Variation with stabilator deflection
$( )_{p}$	Variation with dimensionless roll rate, pb/2U
$( )_{q}$	Variation with dimensionless pitch rate, qc/2U
$( )_{r}$	Variation with dimensionless yaw rate, rb/2U

State Equation Parameters

$A_{lat\text{-}dir}$	Lateral-Directional plant matrix
A_{long}	Longitudinal plant matrix
α	Angle of attack perturbation, radians
β	Sideslip angle perturbation, radians
Φ	Euler angle in roll, radians
ϕ	roll angle perturbation, radians
p	Roll rate perturbation, rad/sec.
Θ	Euler angle in pitch, radians
θ	Pitch angle perturbation, radians

q	Pitch rate perturbation, rad/sec.
r	Yaw rate perturbation, rad/sec.
$X_{lat\text{-}dir}$	Lateral-directional state vector $\left[\beta \; p \; \phi \; r \right]^T$
X_{long}	Longitudinal state vector $\left[\alpha \; q \; \theta \right]^T$
X_{NL}	Nonlinear state vector $\left[\beta \; p \; \Phi \; r \; \alpha \; q \; \Theta \right]^T$

Other Symbols

δs	Stabilator deflection, degrees
λ	Eigenvalue
θ_0	Pitch angle at t=0, radians
AOA	Aircraft angle of attack, degrees or units (as displayed in the cockpit), as specified
$C\theta$, $S\theta$, $T\theta$	Cos(θ), Sin(θ), Tan(θ)
g	Acceleration due to gravity, ft/sec^2
h	Time increment for numerical analysis, sec.
M	Mach number
NATOPS	Naval Air Training and Operating Procedures Standardization
NAVAIR	Naval Air Systems Command
SAS	Stability augmentation system
t	Time, sec.
U_0	Component of freestream velocity along x body axis, ft/sec.

ACKNOWLEDGEMENTS

Special thanks are in order for Joe Gera at NASA Dryden for his guidance and expertise with defining the early stages of this study. Similarly, Fred Schaefer at Grumman was especially helpful in that he acted as my liaison for obtaining and interpreting the data base. His rapid response to many questions and his willingness to discuss at length any topic related to the study are greatly appreciated.

I am deeply indebted to my advisor, Professor Louis Schmidt, who has displayed immeasurable interest in my personal well-being, my career as a student at the Naval Postgraduate School and the development of my career in the years ahead. His enthusiasm, expertise and guidance reignited my interest in flight mechanics and challenged me to pursue this topic in advanced studies. He has provided a nurturing, amiable environment in which professional growth and understanding have come naturally and with great pleasure on my part. It has been an honor to study under his tutelage.

This would not be complete without also expressing thanks to all of the other faculty members who have influenced and shaped my career here at NPS. Along these lines, special thanks to CDR. Mike Daniel, USN (Ret.), who helped me through some difficult times while serving as the curricular officer.

I must also acknowledge my parents, brothers and sister and their families for supporting me during this rather lengthy undertaking. All the "little things" that they have done which are so often taken for granted are very much appreciated.

Lastly, extra special thanks are reserved for my wife and young son who together have had to sacrifice a great many things while supporting me in the pursuit of my graduate education. Without their kindness, love and understanding, this project would never have left the ground.

I. INTRODUCTION

Much has been written on the subject of linearized aircraft flight mechanics. Under the assumption of small perturbations, the equations of motion representing rigid body aircraft dynamics can be reduced to two sets of uncoupled, linear differential equations with constant coefficients which can be readily solved to yield characteristic frequencies, damping ratios, and amplitude/phase relationships of the aircraft's "natural modes", as well as time history traces of aircraft response to these modes due either to initial conditions or control inputs. The approximations made in the analysis of the linearized equations are quite good as long as the aircraft motion is analyzed within the boundaries of linear behavior (i.e., small angles). Under the assumptions made in this relatively benign region, the longitudinal aircraft motions are isolated from the lateral-directional motions. Analytical results from linearized theory agree well with flight tests in this regime, with negligible coupling occurring in flight. As good as these approximations are, they break down completely at high angle of attack, sideslip angle or high angular rates and fail to provide accurate results when analyzed in this manner. Thus, the full set of nonlinear, coupled equations of motion must be analyzed to obtain adequate results. Whereas the motion and inertially related nonlinear terms were neglected in small perturbation theory, these terms provide coupling between the longitudinal and lateral-directional dynamics in the nonlinear analysis, altering the overall dynamic response.

The differences between linear and nonlinear flight dynamics described above form the foundation for this study. In particular, this analysis probes into

the nonlinear phenomena known as wing rock. Numerous studies conducted over recent years in an attempt to identify the specific cause(s) of wing rock have highlighted aerodynamic hysteresis [Ref. 1], complex asymmetric vortex interactions for slender deltas [Ref. 2, 3] and inertial cross coupling [Ref. 4] as potential candidates for the wing rock motion. The validity of these studies is certainly not under question; however, not one of them can be chosen as the specific cause for wing rock in any aircraft without careful consideration due to the highly configuration-dependent nature of the problem. It is with this in mind that this study investigated the effects of inertial cross coupling as a contributor to the wing rock motion in the F-14A aircraft. Although wing rock has been reported in many other aircraft (e.g., A-4, F-4, F-5, [Ref. 1]; HP-115 [Ref. 2]; T-38 [Ref. 4]; F-15 [Ref. 5]; F/A-18, X-29 [Ref. 6]) this aircraft was modeled for a variety of reasons. Perhaps most important among these reasons was the rapidly growing emphasis on high angle of attack research and technology, along with its potential impact on the future combat capability of the F-14. The very existence of aircraft currently displaying excellent high angle of attack performance such as the F-16, F/A-18, and Mig-29 merely suggest that future designs will display even greater capability in this regime. As the F-14 enters its third decade of service, it carries with it a battle-proven record of superior performance. But the realities of reduced military spending and a huge federal deficit make it all too clear that every weapon system in the inventory will be used to the very end of its service life (and as we are witnessing with A-6's, at times beyond the projected service life by sending aircraft through rework facilities for structural repair and/or enhancement; a less time consuming and less expensive alternative to development, test and acceptance of new designs).

Thus, if trends in the defense contracting industry and weapons procurement branches of the armed services continue to proceed as they have in the 80's, it is not unreasonable to assume that the F-14 will remain in service for the foreseeable future, meaning at least into the 21st century. The F-14 will undoubtedly face aircraft with superior high angle of attack capability and may be forced, depending on rules of engagement, current tactics, etc., to fight these aircraft in the high AOA regime. Even with the current upgrades to engines and avionics, the basic airframe of the F-14 will remain the same. Therefore, the dynamic behavior of the aircraft from a stability standpoint will also remain unchanged unless alterations are made to the aircraft's stability augmentation system. If an F-14 experiences wing rock while engaged in an aerial encounter, especially at very high angle of attack, the only current recourse is to neutralize lateral and directional controls and momentarily reduce the angle of attack. Obviously, this course of action may compromise the aircraft and prove to be unrecoverable for the crew. If it is within our means to understand this phenomenon, then we are that much closer to providing and implementing a solution in the form of control laws to avoid it.

Another important reason for studying the F-14 was the relatively simple flight control system incorporated into its design. As opposed to many of the newest high performance aircraft, the F-14 flight control system uses only pilot input via mechanical linkages and a three axis stability augmentation system (SAS) to control the aircraft during normal maneuvering. The aircraft can be flown freely within its envelope without pitch SAS and is restricted to roll SAS off above 15 units AOA for subsonic maneuvering. Thus, only the function of the yaw SAS, the most critical of the three, was of concern to this study.

Although one design feature of the yaw SAS was to provide increased directional stability at high angle of attack, the aircraft can still be maneuvered normally without it "if extra care is taken to control yaw excursions with rudder." [Ref. 7:p. IV-11-1] Therefore, conducting an analysis of the stick fixed stability characteristics of this aircraft without knowledge of the details of its stability augmentation system is not unreasonable. For aircraft with "fly-by-wire" flight control systems, the results of a similar stability analysis may vary by a wider margin (from actual aircraft response) due to the influence of the flight control computer on the control surfaces in response to changing flight conditions, even with no pilot input.

The F-14 also proved to be an excellent choice due to the availability of an extensive aerodynamic data base. Lastly, an abundance of pilot reports from fellow aviators at NPS was readily available.

In an effort to ultimately obtain numerically derived time history traces illustrating wing rock for the F-14, the sections that follow provide a brief background on F-14 high AOA flight characteristics, the aerodynamic data base from which the aircraft stability derivatives were obtained and a summary of the equations of motion. The study continues by describing the numerical procedures used, then highlights the linearized and nonlinearized results. A number of recommendations for related research are presented following the conclusions.

II. F-14A FLIGHT CHARACTERISTICS REVIEW

A. NATOPS FLIGHT MANUAL REVIEW

The F-14A NATOPS Flight Manual [Ref. 7] mentions wing rock and coupling tendencies in the Flight Characteristics section of the manual. The following quotations from the manual are provided to familiarize the reader with the nonlinear dynamics of this aircraft.

> Coupling occurs when motions in more than one axis interact. The F-14A, like all high-performance airplanes capable of producing high rated, multiple axes motion, is susceptible to coupling. High rate, multiple axes motions particularly at high AOA can produce violent coupled departures. [Ref. 7:p. IV-11-18]

> Although the maneuver slats increase the severity of the wing rock between 20 and 28 units AOA, overall departure resistance of the aircraft is greatly improved. The wing rock may be damped with rudders, but greater difficulty may be encountered with maneuver slats, especially at low airspeeds. If this occurs, the wing rock may be damped by neutralizing the lateral and the directional controls and momentarily reducing AOA to below 20 units. [Ref. 7:p. IV-11-7]

> At 20 to 28 units AOA, reduced directional stability is apparent, and even small control inputs will cause yaw oscillations that, if unchecked, can produce a mild wing rock (+/- 10 to 15 degrees).... Wing rock at 20 to 28 units AOA will be more severe (+/- 25 degrees) and more difficult to damp with maneuver slats extended (due to increased dihedral effect). [Ref. 7:p. IV-11-11]

In the takeoff and landing configuration, wing rock is also experienced at high AOA during approach to stall, as indicated by the following excerpt from the NATOPS.

> At 25 units AOA divergent wing rock and yaw excursions define the stall. Sideslip angle may reach 25 degrees, and bank angle 90 degrees within 6 seconds if AOA is not lowered.... Extending the speed brakes ... improves directional stability significantly, reducing the wing rock and yaw tendency at 25 units AOA. Stall approaches should not be continued beyond the first indication of wing rock. When wing rock occurs, the nose should be lowered and no attempt should be made to counter the wing rock with lateral stick or rudder. [Ref. 7:p. IV-11-18]

B. FLIGHT TEST TIME HISTORIES

To further illustrate the characteristics of wing rock for this aircraft, several time history traces from two actual flight tests are shown in Figures 1a-1d and 2a-2d [Ref. 8]. In both sets, it can be noted that the lateral acceleration of the c.g. shown in Figures 1d and 2d can be converted into a sideslip perturbation.

The first set of traces, Figures 1a-1d, was obtained from a flight test conducted at approximately 20,000 ft., Mach .32, with maneuver flaps extended, wings swept fully forward and the SAS off. The initial angle of attack (ARI ALPHA) from the plot was 14 degrees. This angle corresponded to approximately 12 degrees true AOA via the conversion

$$AOA_{true} = .8122*AOA_{ARI} + .7971 \qquad (01)$$

[Ref. 8] and 17 units indicated AOA via the conversion

$$AOA_{units} = 1.0989 * (AOA_{true} + 3.01) \qquad (02)$$

which is valid for the F-14 operating at Mach number less than .4 [Ref. 9].

As the time history began, the aircraft was decelerating and most likely experiencing light buffet (note the rapid variations in normal acceleration, Figure 1a). In order to maintain altitude, the pilot commanded aft stick. This input resulted in corresponding increases in stabilator position, angle of attack and pitch attitude (Figure 1b). Around 15 seconds and at the equivalent of approximately 18.5 units AOA, very slight roll rate oscillations began which resulted in a 20 degree left wing down attitude after about 28 seconds and coupled into small angle of attack and sideslip perturbations. The pilot responded with a slight right stick correction towards wings level, at which time larger roll rate and roll amplitude oscillations began to develop, at around 30-35 seconds (Figure 1c). The angle of attack at the point where pronounced wing rock oscillations first appeared was the equivalent of 20.5 units. At the same time, larger sideslip and yaw rate oscillations began to appear (Figure 1d), as well as a rapid nose down pitch rate. As the left wing down oscillations were arrested and the mean value of the wing oscillation returned towards wings level, the lateral stick input was taken out. With the decrease in pitch attitude came a loss in altitude and an increase in velocity. Recovery began by applying forward stick to reduce angle of attack at about 45 seconds, although the oscillations continued beyond the end of the trace at 60 seconds.

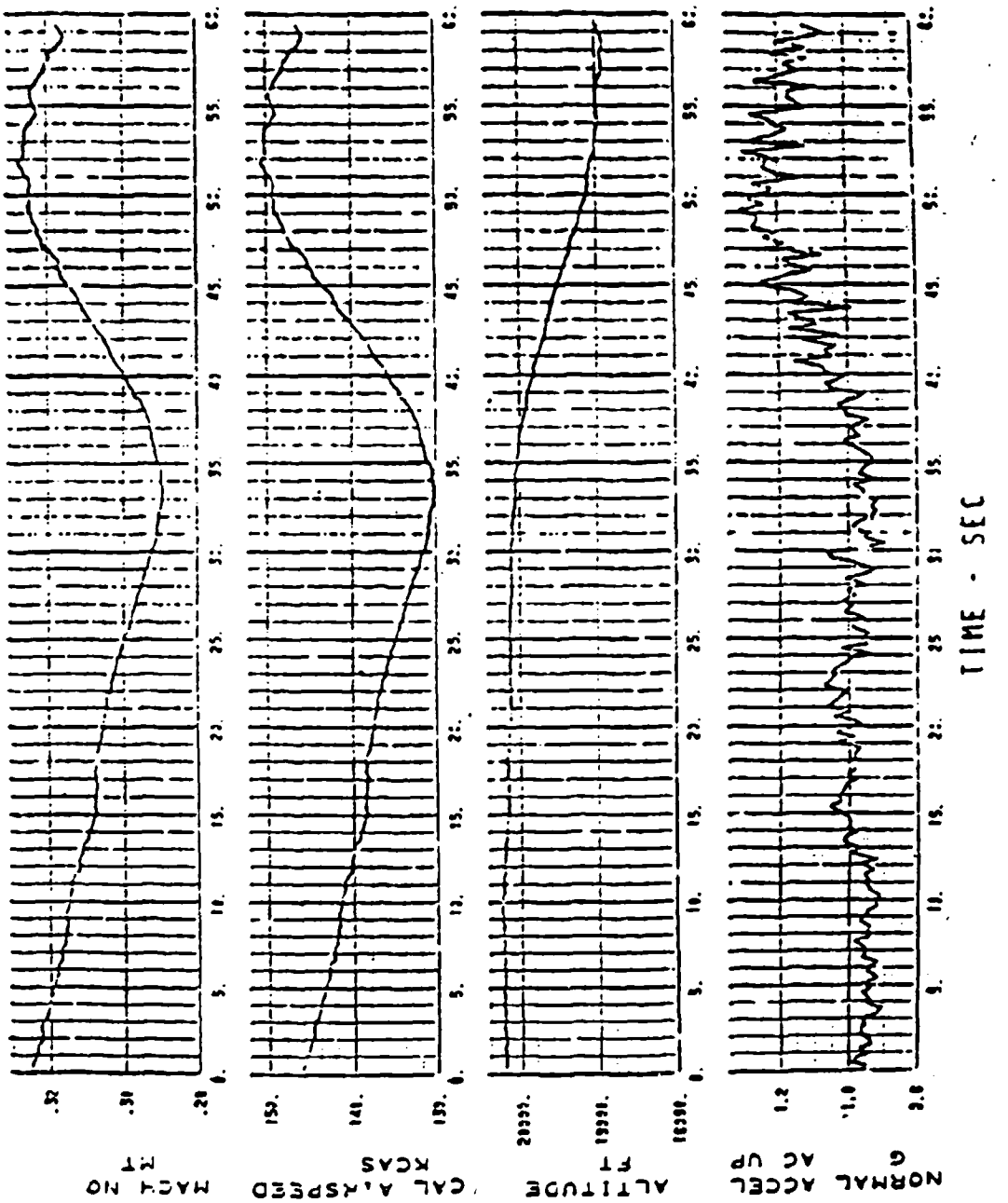

Figure 1a. Flight Test Time History Traces

F-14A 1X, BUNO 157991, FLT 264, GW 55386 LB., C.G. 6.8 % MAC

SWEEP=19 DEG, FLAPS=11 DEG, ALT=20200 FT, MACH .32, SAS OFF

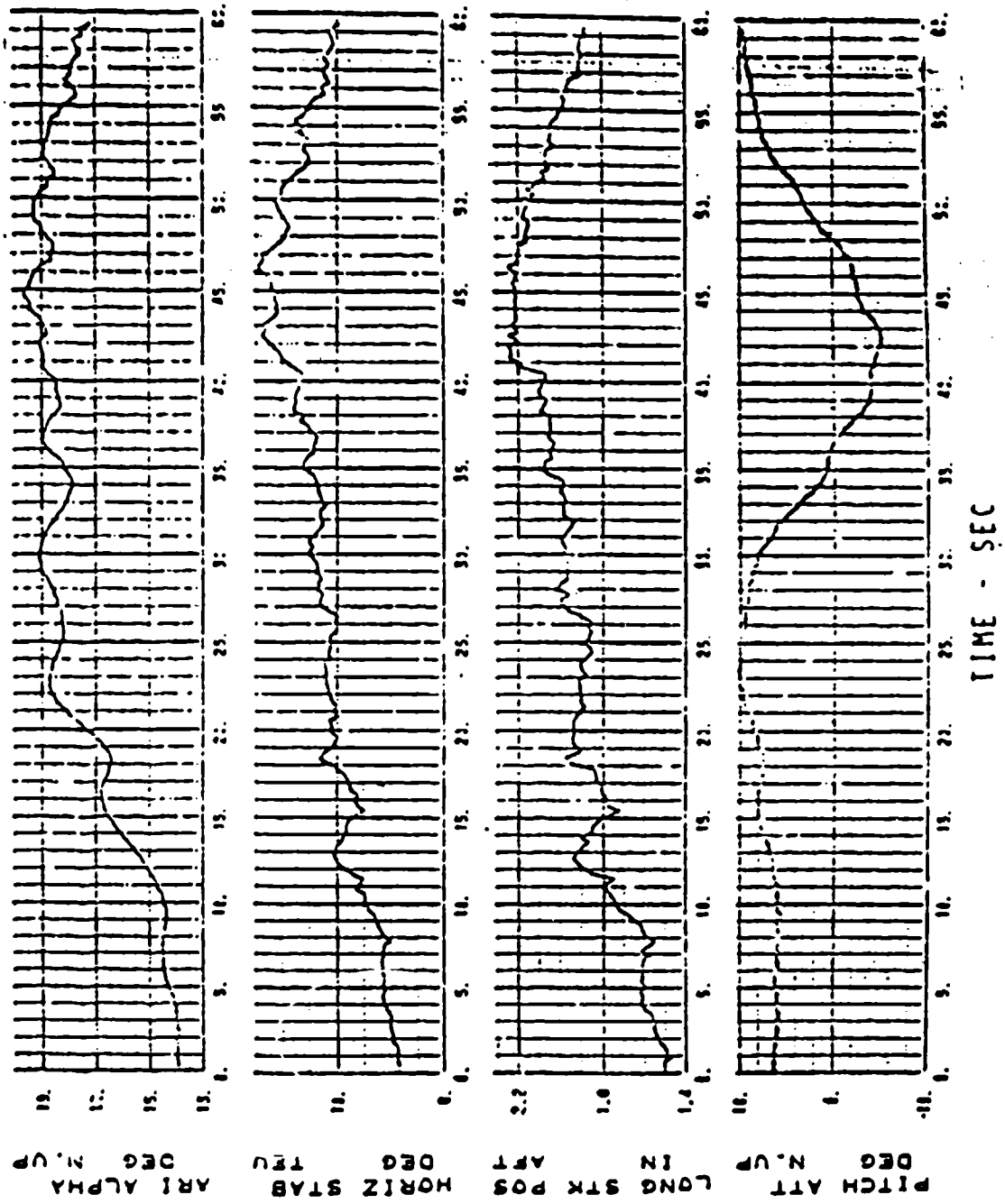

Figure 1b. Flight Test Time History Traces

F-14A 1X, BUNO 157991, FLT 264, GW 55386 LB., C.G. 6.8 % MAC

SWEEP=19 DEG, FLAPS=11 DEG, ALT=20200 FT, MACH .32, SAS OFF

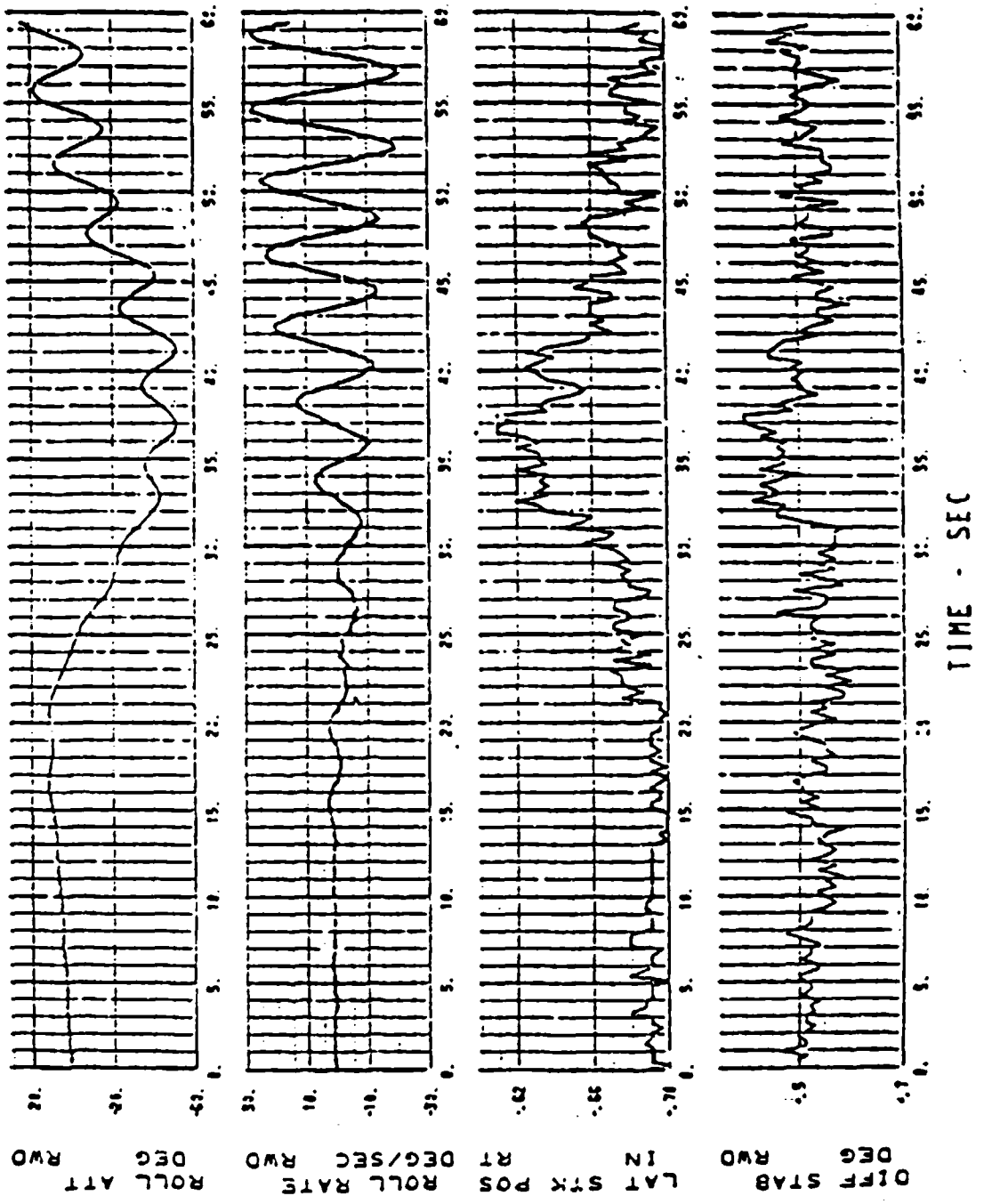

Figure 1c. Flight Test Time History Traces

F-14A 1X, BUNO 157991, FLT 264, GW 55386 LB., C.G. 6.8 % MAC

SWEEP=19 DEG, FLAPS=11 DEG, ALT=20200 FT, MACH .32, SAS OFF

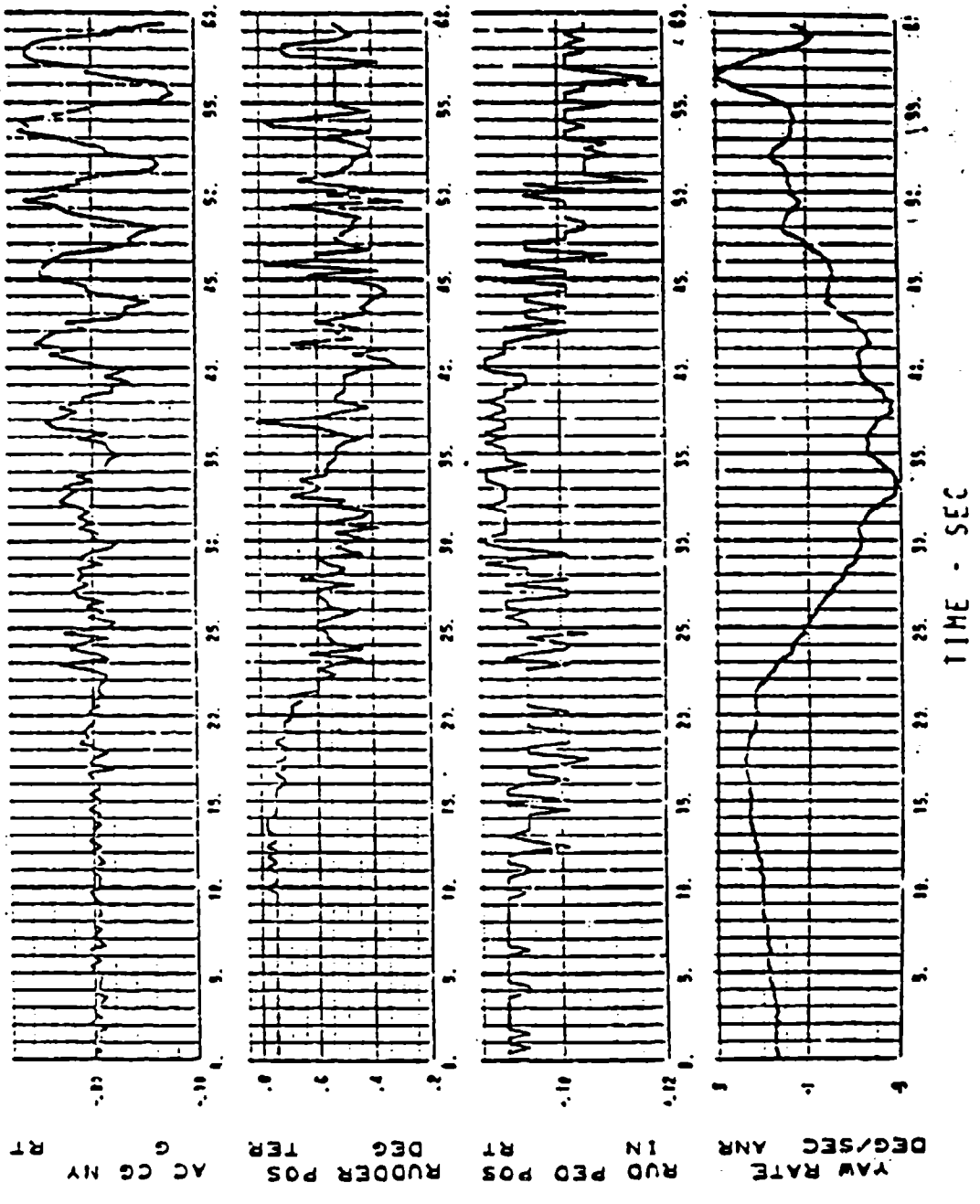

Figure 1d. Flight Test Time History Traces

F-14A 1X, BUNO 157991, FLT 264, GW 55386 LB., C.G. 6.8 % MAC

SWEEP=19 DEG, FLAPS=11 DEG, ALT=20200 FT, MACH .32, SAS OFF

The second set of traces, Figures 2a-2d, was taken from the same test flight at a nearly identical flight condition, except that the altitude was approximately 19,000 ft. The initial angle of attack (ARI ALPHA) from the plot was 17 degrees. This corresponded to approximately 14.5 degrees true AOA and 19.5 units as seen in the cockpit. In this demonstration, the aircraft began by quickly decelerating and increasing AOA to 19 degrees ARI (approximately 16.5 degrees true and 21 units, Figures 2a and 2b). The immediate presence of roll and roll rate oscillations without lateral control inputs is evident in Figure 2c, as well as sideslip and yaw rate oscillations in Figure 2d. The roll amplitude eventually reached approximately +/- 45 degrees with a period of about 5 seconds. It is evident that frequency doubling in the AOA perturbation occurred, as the period was about 2-2.5 seconds. The AOA reached approximately 25.5 units at its highest point. Also, a pronounced decrease in pitch angle was evident once small AOA perturbations appeared at around 10 seconds. Furthermore, loss of altitude appeared as the roll angle oscillations built beyond +/- 30 degrees from the mean value at around 25 seconds.

All of these illustrations clearly indicate that the motions which occur at high angle of attack are quite complex and that nonlinear coupling occurs between the longitudinal and lateral-directional equations of motion.

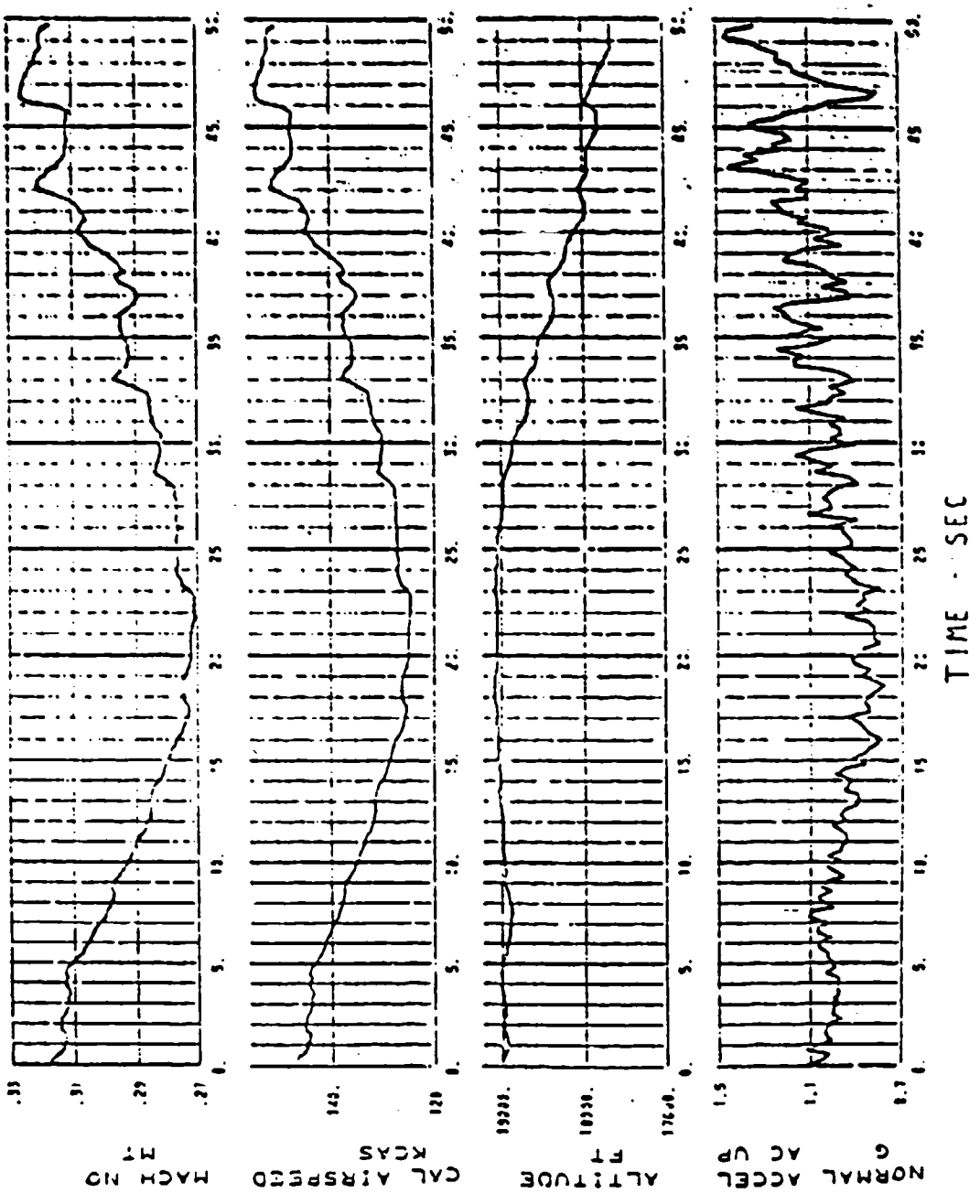

Figure 2a. Flight Test Time History Traces

F-14A 1X, BUNO 157991, FLT 264, GW 55345 LB., C.G. 7.1 % MAC

SWEEP=19 DEG, FLAPS=11 DEG, ALT=18988 FT, MACH .32, SAS OFF

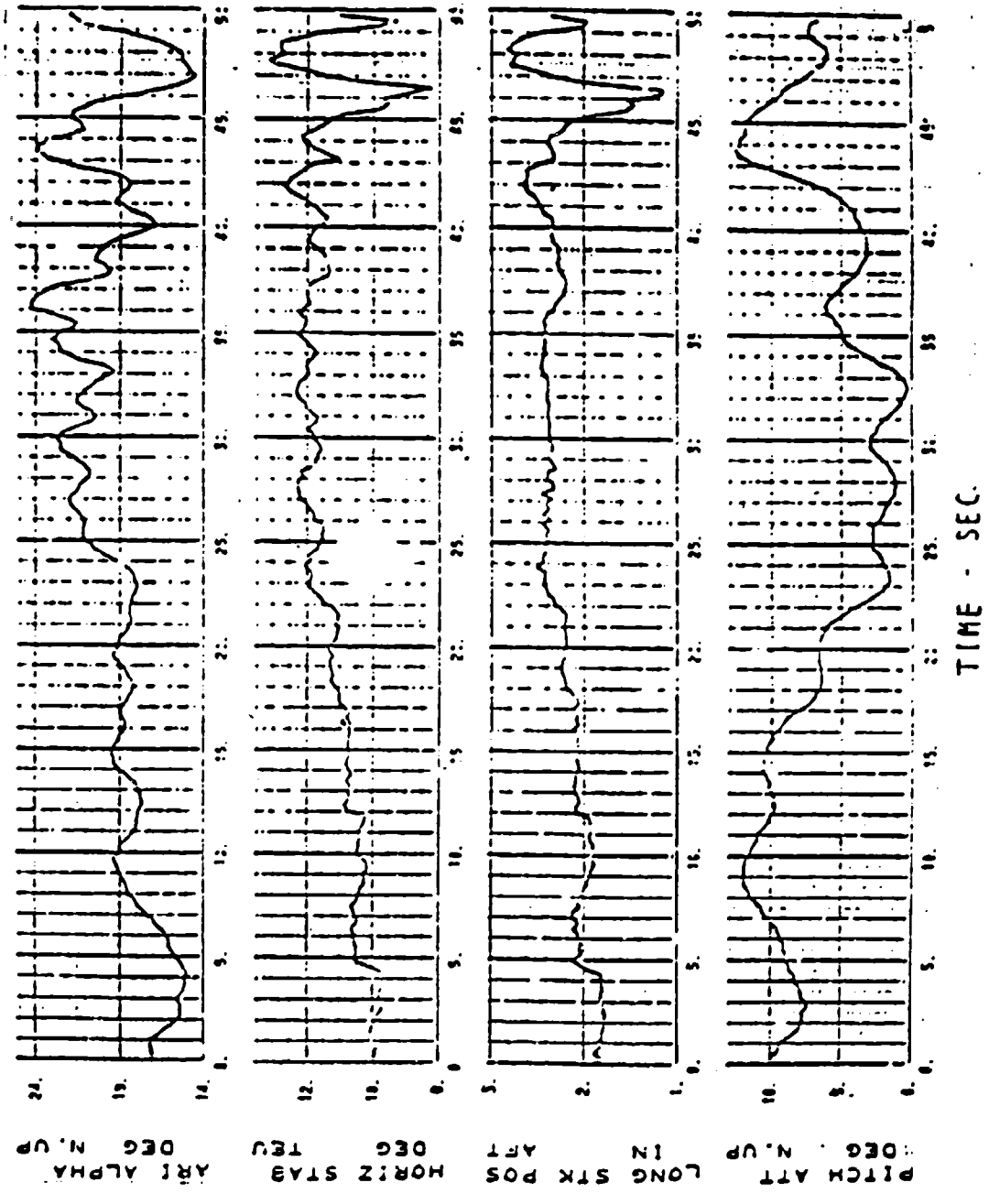

Figure 2b. Flight Test Time History Traces

F-14A 1X, BUNO 157991, FLT 264, GW 55345 LB., C.G. 7.1 % MAC

SWEEP=19 DEG, FLAPS=11 DEG, ALT=18988 FT, MACH .32, SAS OFF

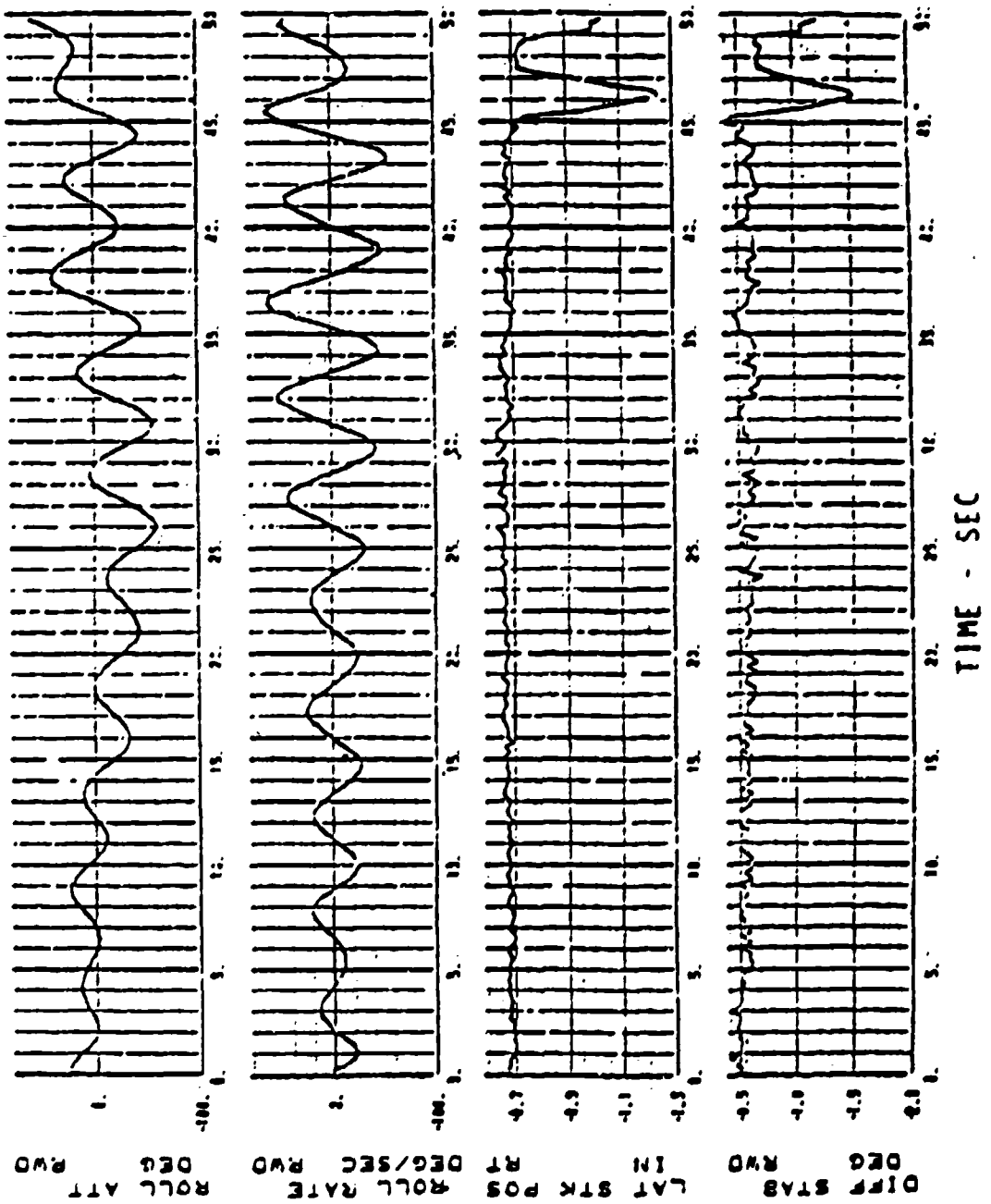

Figure 2c. Flight Test Time History Traces

F-14A 1X, BUNO 157991, FLT 264, GW 55345 LB., C.G. 7.1 % MAC

SWEEP=19 DEG, FLAPS=11 DEG, ALT=18988 FT, MACH .32, SAS OFF

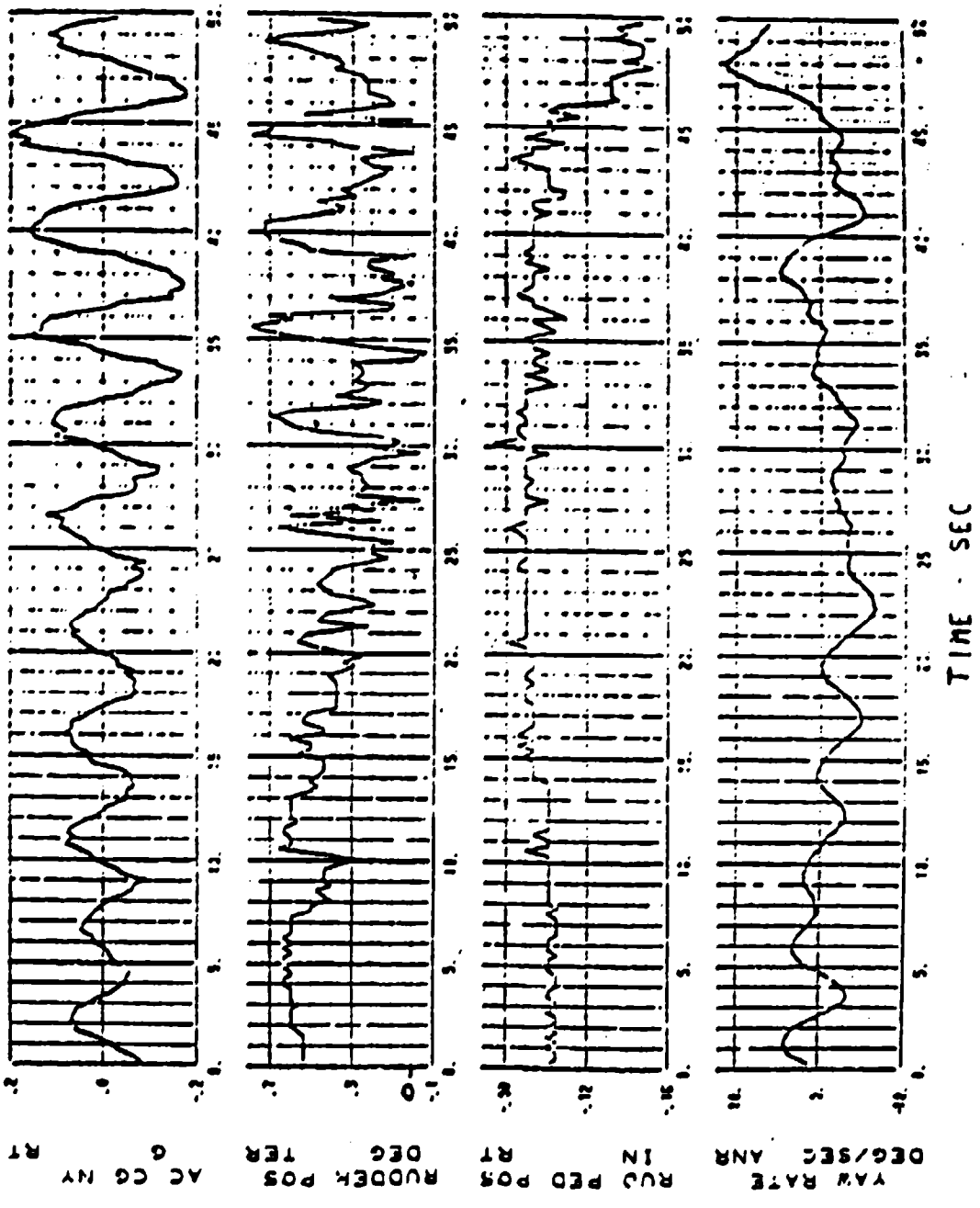

Figure 2d. Flight Test Time History Traces

F-14A 1X, BUNO 157991, FLT 264, GW 55345 LB., C.G. 7.1 % MAC

SWEEP=19 DEG, FLAPS=11 DEG, ALT=18988 FT, MACH .32, SAS OFF

III. A DESCRIPTION OF THE AERODYNAMIC DATA BASE

The stability derivatives needed to obtain the coefficients in the equations of motion for the F-14 came from an aerodynamic data base provided by the Grumman Corporation, Bethpage, New York [Ref. 9]. The data base consisted of aerodynamic and stability coefficients from wind tunnel and spin tunnel tests conducted on a flight test aircraft at the NASA Langley Research Facility. The tabulated data represented two different flight regimes; a low speed regime where Mach number remained at or below M=.6 and a high speed regime for Mach number greater than M=.6. Typically, the low speed data appeared in the tables as a function of angle of attack and sideslip, although some stability derivative coefficients were dependent solely on AOA, while others were dependent upon AOA, sideslip and control surface deflection. All data in the tables was referenced to the body axis coordinate system (x - axis corresponding to the aircraft's longitudinal axis). Therefore, coordinate transformations through the angle of attack were required to obtain coefficients related to lift and drag. Additionally, crossplots, curve fits and a number of other techniques were employed to obtain all of the necessary information for the stability analysis. A detailed description of the techniques used to obtain the stability parameters from the wind tunnel data appears in Appendix A.

It is very important to remember the distinction between true angle of attack expressed in degrees and in units. The conversion between degrees true and units for the F-14 at Mach number less than .4 was given in equation (02). The net effect of this conversion is to subtract five from the indicated AOA expressed in units to get AOA in degrees (i.e., 25 units = 20 degrees). This distinction

should be kept in mind when comparing the NATOPS flight characteristics to the results of this study, which indicate aircraft response at various true angles of attack expressed in degrees.

IV. EQUATIONS OF MOTION DEVELOPMENT

The equations of motion describing the dynamic behavior of an aircraft are typically developed in a rotating reference frame fixed to the aircraft's body axes. The aircraft is assumed to be a rigid body, such that aeroelastic and gyroscopic effects are neglected. Additionally, the variation in aircraft velocity is assumed to be negligible for the purposes of this study. This approximation allows for the removal of the X force equation and the perturbation velocity from the longitudinal equations of motion. After the assumption of small perturbations is made and the linearization of the equations is completed, they can be conveniently expressed in state space format as shown below.

$$\dot{X}_{long} = A_{long} X_{long} \tag{03}$$

and

$$\dot{X}_{lat\text{-}dir} = A_{lat\text{-}dir} X_{lat\text{-}dir} \tag{04}$$

where

$$X_{long} = \begin{bmatrix} \alpha & q & \theta \end{bmatrix}^T \tag{05}$$

$$A_{long} = \begin{bmatrix} \frac{Z_\alpha}{U} & 1 & \frac{-g\sin\theta_0}{U} \\ M_\alpha' & M_q' & 0 \\ 0 & 1 & 0 \end{bmatrix} \tag{06}$$

$$M_\alpha' = M_\alpha + \frac{1}{U}(M_{\dot{\alpha}} Z_\alpha) \tag{07}$$

$$M_q' = M_q + M_{\dot{\alpha}} \tag{08}$$

$$X_{lat\text{-}dir} = \begin{bmatrix} \beta & p & \phi & r \end{bmatrix}^T \tag{09}$$

$$A_{lat\text{-}dir} = \begin{bmatrix} \frac{Y_\beta}{U} & 0 & \frac{g\cos\theta_0}{U} & -1 \\ L_\beta & L_p & 0 & L_r \\ 0 & 1 & 0 & 0 \\ N_\beta & N_p & 0 & N_r \end{bmatrix} \tag{10}$$

This method of describing the governing equations is compact and readily shows that the longitudinal and lateral-directional equations for the linearized case are uncoupled. It also lends itself to matrix operations for determining the stability characteristics of the natural modes for both longitudinal and lateral-

directional motion. A general description of the natural modes normally associated with small perturbation theory is presented in Etkin [Ref. 10]. The dimensional derivatives which make up the elements of A_{long} and $A_{lat\text{-}dir}$ are in accordance with NASA convention and are defined in McRuer, Ashkenas and Graham [Ref. 11].

When the underlying assumptions of small perturbation theory are extended in order to introduce non-linear terms in the equations of motion, the linearized equations shown above must be modified to account not only for the extra non-linear terms, but also to drop out the terms resulting from the linearization. Additionally, Euler angle relations are introduced so that the roll angle ϕ becomes the Euler angle Φ and the pitch angle θ becomes the Euler angle Θ. The additional terms to be added to transform the linearized equations into the fully coupled, non-linear equations are shown below.

$$(NL)_\beta = p\alpha + \frac{g}{U}(C_\theta S_\phi - C_{\theta_0}\phi) \tag{11}$$

$$(NL)_p = \frac{I_y - I_z}{I_x}\, qr \tag{12}$$

$$(NL)_\phi = (qS_\phi + rC_\phi)\, T_\theta \tag{13}$$

$$(NL)_r = \frac{I_x - I_y}{I_z}\, qp \tag{14}$$

$$(NL)_\alpha = -p\beta + \frac{g}{U}(C_\theta C_\phi - C_{\theta_0} + S_{\theta_0}\theta) \tag{15}$$

$$(NL)_q = \frac{I_z - I_x}{I_y}\, rp + M_{\dot{\alpha}}(NL)_\alpha \tag{16}$$

$$(NL)_\theta = q(C_\phi - 1) - rS_\phi \tag{17}$$

and the new state vector for the non-linear equation set is:

$$X_{NL} = \left[\beta \quad p \quad \Phi \quad r \quad \alpha \quad q \quad \Theta \right]^T \tag{18}$$

It will be noted that the aerodynamic terms still retain their linear form while the nonlinear aspects are introduced via inertial coupling. Retaining the simplified forms for the aerodynamic terms is deliberate at this stage of the analysis in order to illustrate the influence of inertial coupling upon the ensuing motion response.

V. COMPUTATIONAL PROCEDURES

A. LINEAR SYSTEMS OF EQUATIONS

An understanding of the equations of motion and the significance of their nonlinearity is essential prior to attempting to determine the aircraft's response to an initial perturbation. Had the equations remained purely linear, a relatively simple solution would have been available by calculating the eigenvalues of the characteristic polynomial and each associated eigenvector. The general solution of a linear differential equation is a linear combination of all linearly independent solutions. Therefore, the general solution can be expressed explicitly as a function of time as follows (two degree of freedom system shown for clarity):

$$\{x(t)\} = c_1 \{x_1\} e^{\lambda_1 t} + c_2 \{x_2\} e^{\lambda_2 t} \qquad (19)$$

where $\{x(t)\}$ is a column vector whose individual components represent the time response of each degree of freedom, λ_1 and λ_2 are the eigenvalues, $\{x1\}$ and $\{x2\}$ are the associated eigenvectors and c_1 and c_2 are constants representing the modal participation of each of the modes in the response. In general, the eigenvalues are complex in nature and represent a damped, oscillatory solution. Utilizing the fundamentals of complex arithmetic as applied to a response with real physical terms, the expression may be rewritten as a combination of sines and cosines to remove the complex terms, thereby leaving the equation as a trigonometric function of time alone. Once the time domain solution is found in

this manner, time history traces may be generated using a short computer algorithm. Such an algorithm might iterate time, calculate the value of each component of {x(t)} at that time, store the values in a data file and repeat the procedure. Plotting the data would provide the time history traces. Although the procedure outlined here was intended to iilustrate the ease with which a purely linear system can be solved, the technique described in the next section was used to solve both the linear and nonlinear systems of equations so that only one program had to be used regardless of the desired form of the solution. Even so, the calculation of eigenvalues, eigenvectors, natural frequencies and damping ratios remained important and was used extensively in the linear analysis because the character of the dynamic response could be determined and visualized solely by these parameters. The actual time history response provided an added means of visualizing the influence of these parameters.

B. NONLINEAR SYSTEMS OF EQUATIONS

A computer program was used to numerically integrate both the linear and nonlinear equations of motion to obtain a time history response. As mentioned earlier, the algorithm was capable of numerically integrating linear differential equations as well as nonlinear equations. Therefore, the same program was used to obtain either the linear or the nonlinear response, depending on the solution desired.

The heart of the program was a numerical integration technique based on Richardson's extrapolation; an explicit, two-step numerical procedure which can be readily applied to first order differential equations. It is a variation of the

second order Runge-Kutta method. The basic concept behind the method is presented by Ferziger [Ref. 12] and demonstrated by the following example.

Suppose the first derivative of each variable of interest is expressed explicitly as a function of known initial conditions at time t=0. By simple substitution, the numerical value of each derivative can be calculated and used to approximate the value of the variables of interest a short time later. Mathematically,

$$y^{(1)}_{(n+1)} = y_n + h\,\dot{y}_n \tag{20}$$

where h is the time increment, n represents a discretized time step and the superscript (1) denotes that the value of $y_{(n+1)}$ calculated here is just the first estimate of the final value at time $t_{(n+1)} = t_n + h$. The calculation is then repeated using two steps, each at half of the original time increment as shown below.

$$y^{(2)}_{(n+1/2)} = y_n + \frac{h}{2}\,\dot{y}_n \tag{21}$$

$$y^{(2)}_{(n+1)} = y_{(n+1/2)} + \frac{h}{2}\,\dot{y}_{(n+1/2)} \tag{22}$$

The superscript (2) indicates that the calculated value is the second estimate of the final value. The estimates are then combined using Richardson's

extrapolation to obtain the final expression for the variable of interest at the new time.

$$y_{(n+1)} = 2\, y^{(2)}_{(n+1)} - y^{(1)}_{(n+1)} \qquad (23)$$

This procedure is repeated for all of the variables at each time step to obtain updated values for each variable at the new time step. The value of each variable at the new time step is then stored in a data file for subsequent plotting. The time is then incremented and the first derivatives recalculated using the updated information from the previous time step. The process continues for a length of time as specified by the user, at which time the computer program terminates. After an investigation to determine the time step required to retain sufficient accuracy was conducted, the time step was set at .05 seconds.

C. INPUTS TO COMPUTER PROGRAM

The program mentioned in the previous section required specific inputs which served to identify the geometry, configuration, inertial properties and aerodynamic characteristics of the aircraft in its trimmed condition. While most of this information remained constant regardless of the angle of attack studied, the aerodynamic characteristics which determine the dynamic response of the aircraft were highly dependent upon, among other things, angle of attack. Therefore, to describe the character of the aircraft in the program at each different angle of attack, the longitudinal and lateral-directional "plants" corresponding to the linear response at the desired trim AOA were used. These "plants" are the square matrices labeled A_{long} and $A_{lat\text{-}dir}$ in equations (06) and

(10) which contain the coefficients in the equations of motion. These coefficients are made up of specific combinations of the stability derivatives which are normally determined by wind tunnel testing and post flight parameter identification techniques. The nonlinear terms were programmed in and selected as a program option if a nonlinear solution was chosen by the user.

In addition to these items, initial conditions were specified to obtain a non-zero response. The choice of initial conditions was important in obtaining a coupled response consistent with the documented response of the aircraft. The choice of initial conditions will be discussed later. A complete listing of the computer program appears in Appendix B.

VI. ANALYSIS

The ultimate goal of this analysis was to obtain multiple time history traces which characterized the aircraft wing rock motion, one trace corresponding to each of the seven pertinent degrees of freedom. In building up to this goal, a linearized analysis (and, therefore, uncoupled as well) was used first to ensure that the aircraft's response to known stabilizing or destabilizing conditions would produce convergent or divergent behavior, respectively. Furthermore, the linear results could be used as a benchmark to compare to the nonlinear, coupled response once that response was determined. The study included aircraft response at angles of attack ranging from zero to 25 degrees so that the variations in the response due to the initial trim condition could be evaluated. A summary of the trim conditions for flight with gear up and flaps at maneuver at 500 ft. appears below in Table 1.

TABLE 1

SUMMARY OF AIRCRAFT TRIM CONDITIONS

AOA (degrees)	AOA (units)	Trim Velocity (ft/sec)	Trim Velocity (kts)	Mach number
0	3.3	575	345	0.52
5	8.8	326	196	0.29
10	14.3	255	153	0.23
15	19.8	228	137	0.20
20	25.3	213	128	0.19
25	30.8	194	116	0.17

The geometric and inertial properties of the aircraft described in the data base were as follows:

$$WT = 52000 \text{ lb.}$$

$$C.G. = 16.2 \% \text{ MAC}$$

$$I_{xx} = 51509 \text{ slug ft}^2$$

$$I_{yy} = 232773 \text{ slug ft}^2$$

$$I_{zz} = 275627 \text{ slug ft}^2$$

$$I_{xz} = 2654 \text{ slug ft}^2$$

It is critically important to recognize that although an aircraft is never flown stick fixed, a stability analysis conducted in this manner provides very useful information on the tendencies of the aircraft to move about its trim position once disturbed. The flying qualities of an aircraft are very much dependent on these stability characteristics. In fact, handling qualities ratings are based on the dynamic characteristics of the linearized modes for many aircraft.

A. LINEAR ANALYSIS

To begin the linear analysis, the characteristic polynomial for both the longitudinal and lateral-directional "plants" were solved for the eigenvalues of each system. The natural frequencies, modal damping and associated eigenvectors were also calculated. As previously mentioned, these parameters serve to identify the character of the dynamic response for each of the natural modes. A summary of the linearized systems short period and dutch roll characteristics is provide below in Table 2.

TABLE 2

SUMMARY OF LINEARIZED DYNAMIC CHARACTERISTICS

	Short Period		Dutch Roll	
AOA (degrees)	Natural Frequency (rad/sec)	Damping Ratio	Natural Frequency (rad/sec)	Damping Ratio
0	1.8729	0.7452	2.5202	0.1067
5	1.0607	0.7488	1.511	0.0755
10	0.8116	0.7352	1.3056	-0.0087
15	0.6725	0.6642	1.0416	-0.1727
20	0.6206	0.6716	1.0138	-0.3575
25	0.5602	0.6766	0.7061	-0.4725

A quick look at this table reveals a great many things about the character of the aircraft's dynamic response at the angles of attack studied. The following paragraphs provide an in depth discussion of the linearized results for the F-14A.

1. Short Period Mode

a. Time History Response

The F-14 displays a stable, heavily damped short period mode at all of the angles of attack studied in this analysis. When excited, this mode tends to produce a rapidly convergent solution back to the initial trim condition. The short period response for zero degrees angle of attack is shown below in Figure 3. The short period responses for the other angles of attack are not shown due to their similarity to the AOA=0 response.

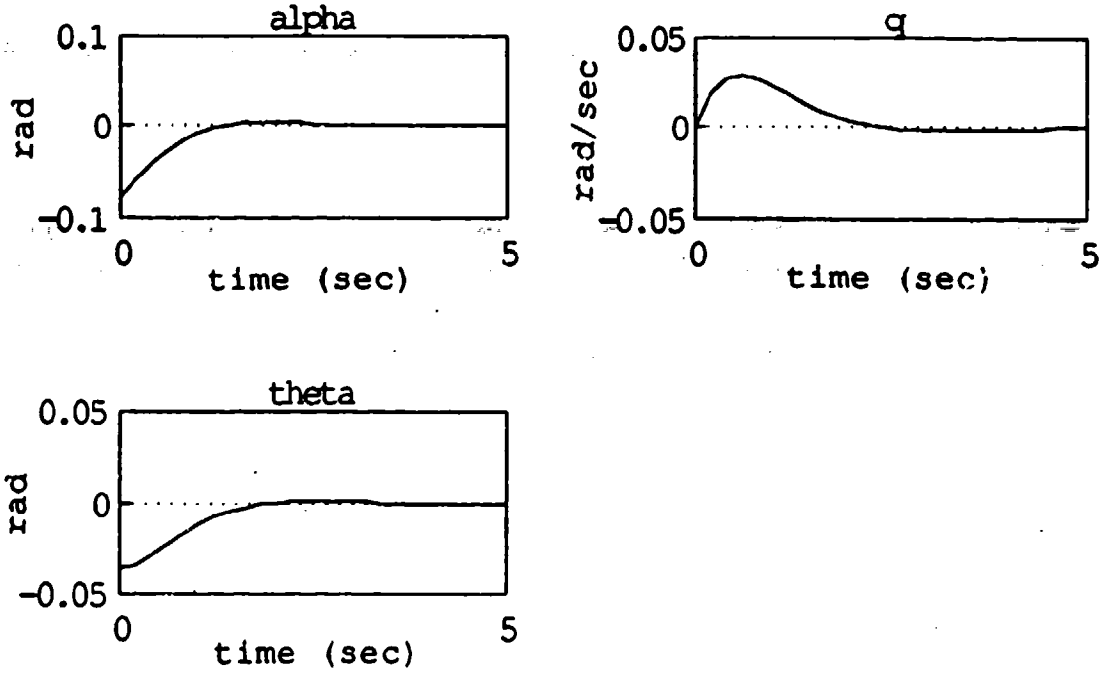

Figure 3. Short Period Response for AOA = 0 degrees

The initial conditions used to generate the short period response corresponded to a one-tenth scaling of the normalized complex eigenvector at t=0. The normalized eigenvector was scaled in this manner to produce an initial perturbation quantity consistent with the magnitudes expected in flight. This technique took into account the phase relationship between each component of the eigenvector and produced the true physical relationship between each component at any time.

b. Root Locus

It is interesting to note the changing position of the characteristic roots (eigenvalues) of the longitudinal system as angle of attack changes. The

migration of the roots has a large impact on the character of the dynamic response in that the natural frequency and damping ratio are determined by the location of the roots in the complex plane. Shown below in Figure 4 is a root locus showing the migration of the short period roots.

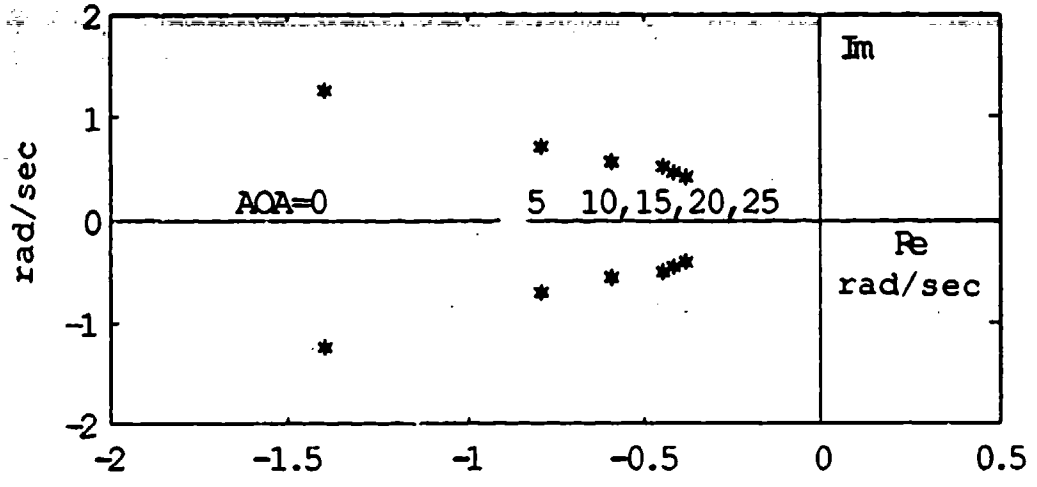

Figure 4. Short Period Root Locus

2. Dutch Roll Mode

The F-14 displays an unstable dutch roll mode at high angle of attack due in part to degraded directional stability ($C_{n\beta}$ going positive to negative) which appears at around 15-20 degrees AOA, depending on aircraft speed and external stores loading. The Out of Control Flight Training Guide [Ref. 13] illustrates this degradation with speed and external loading as shown in Figures 5 and 6. The variation of the directional stability parameter $C_{n\beta}$ calculated from the data base is shown in Figure 7. The increase in dihedral effect ($C_{l\beta}$ getting more negative) and the decrease in roll damping (C_{lp} getting less negative) as angle of attack increases also contribute significantly to the dutch roll instability.

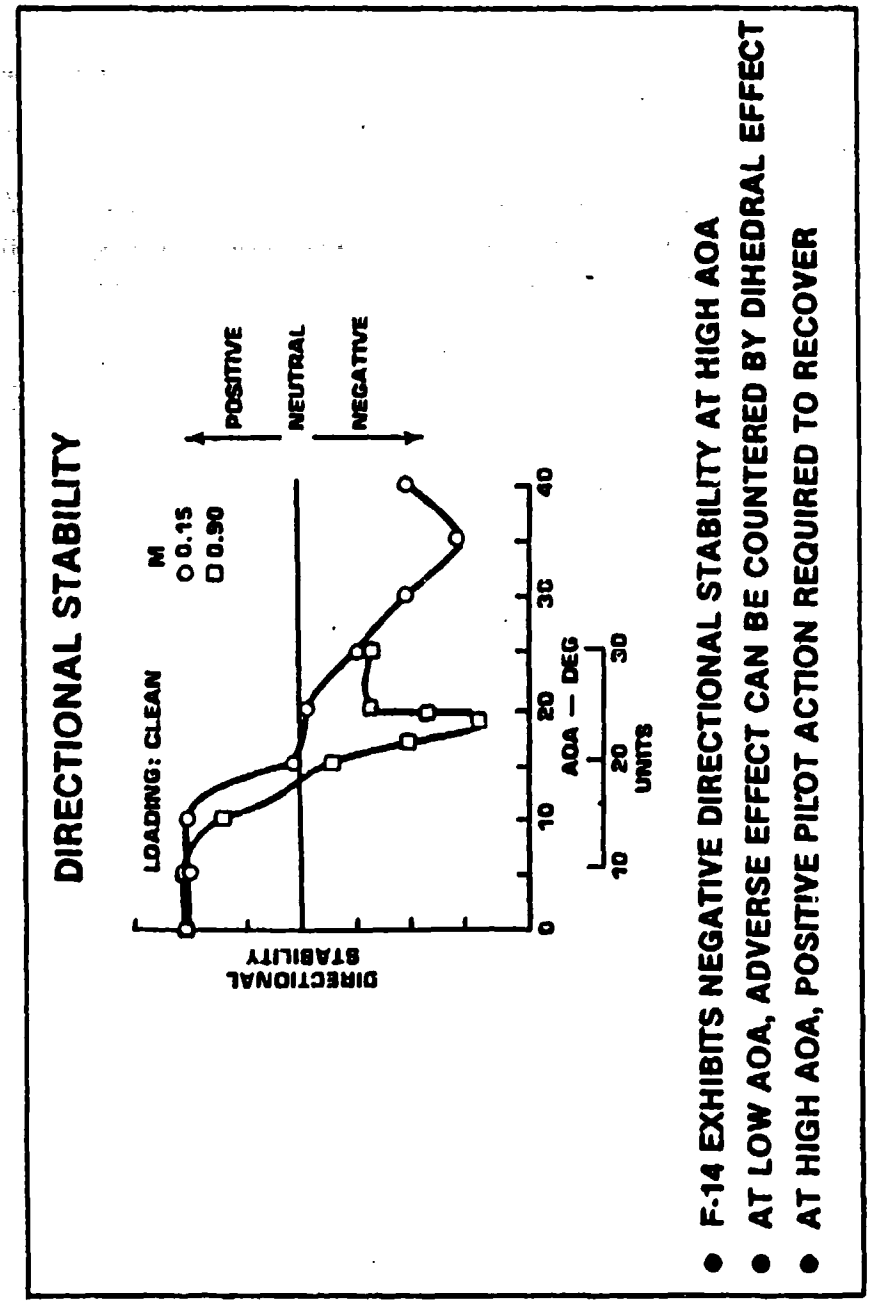

Figure 5. Influence of Speed on Directional Stability

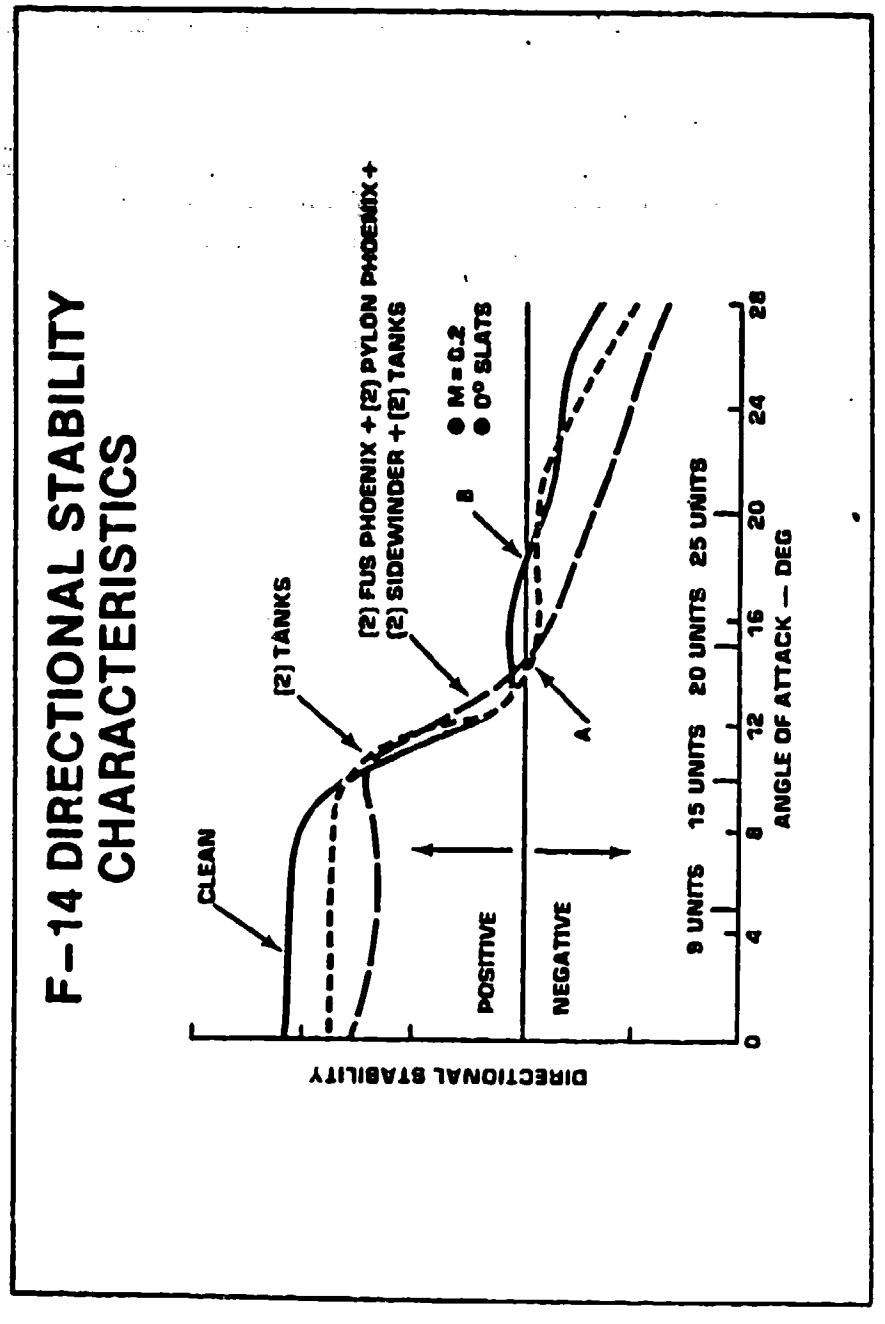

Figure 6. Influence of External Stores on Directional Stability

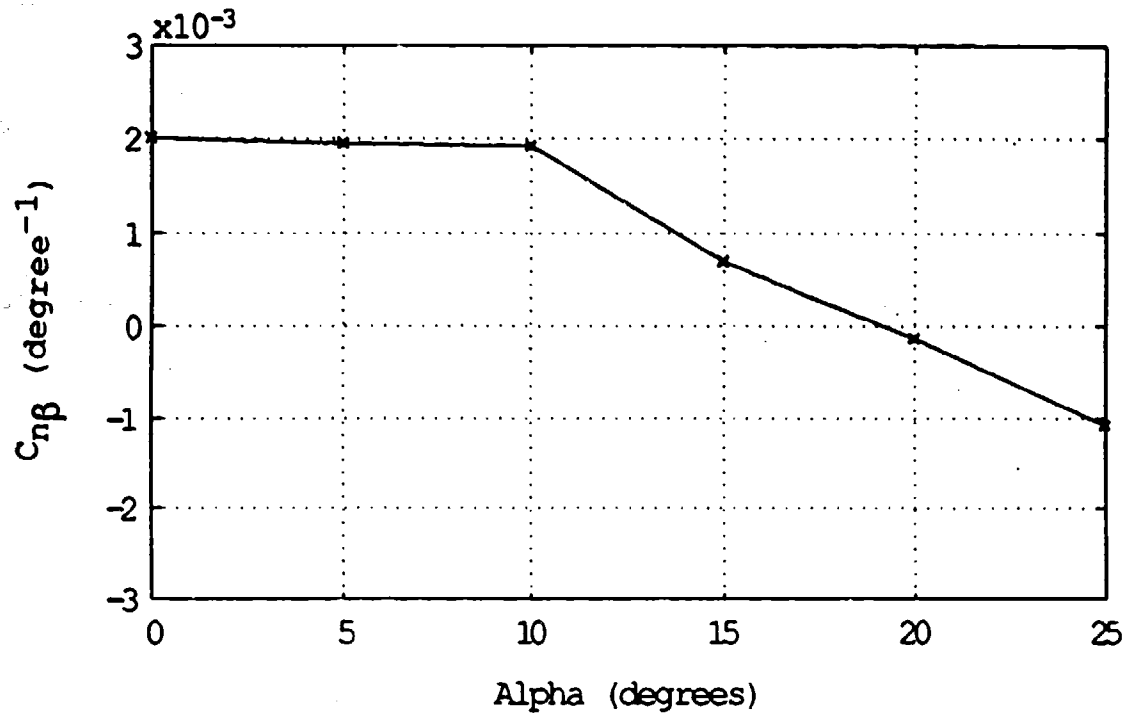

Figure 7. Variation of $C_{n\beta}$ with Angle of Attack from Database

When this unstable mode is excited, the aircraft tends to diverge unless pilot inputs are made to control the motion.

a. Time History Response

The linear analysis reveals that the dutch roll mode is lightly damped at low angles of attack. This results in a slowly convergent oscillation for both zero and five degrees angle of attack. As angle of attack increases past ten degrees, the dutch roll mode goes unstable. At this point it is only slightly unstable, resulting in a very slow divergent oscillation. As angle of attack continues to increase, the dutch roll mode becomes extremely unstable, resulting in a rapid divergence. Figures 8, 9 and 10 show the dutch roll time history responses for AOA=0, 10 and 15 degrees, respectively.

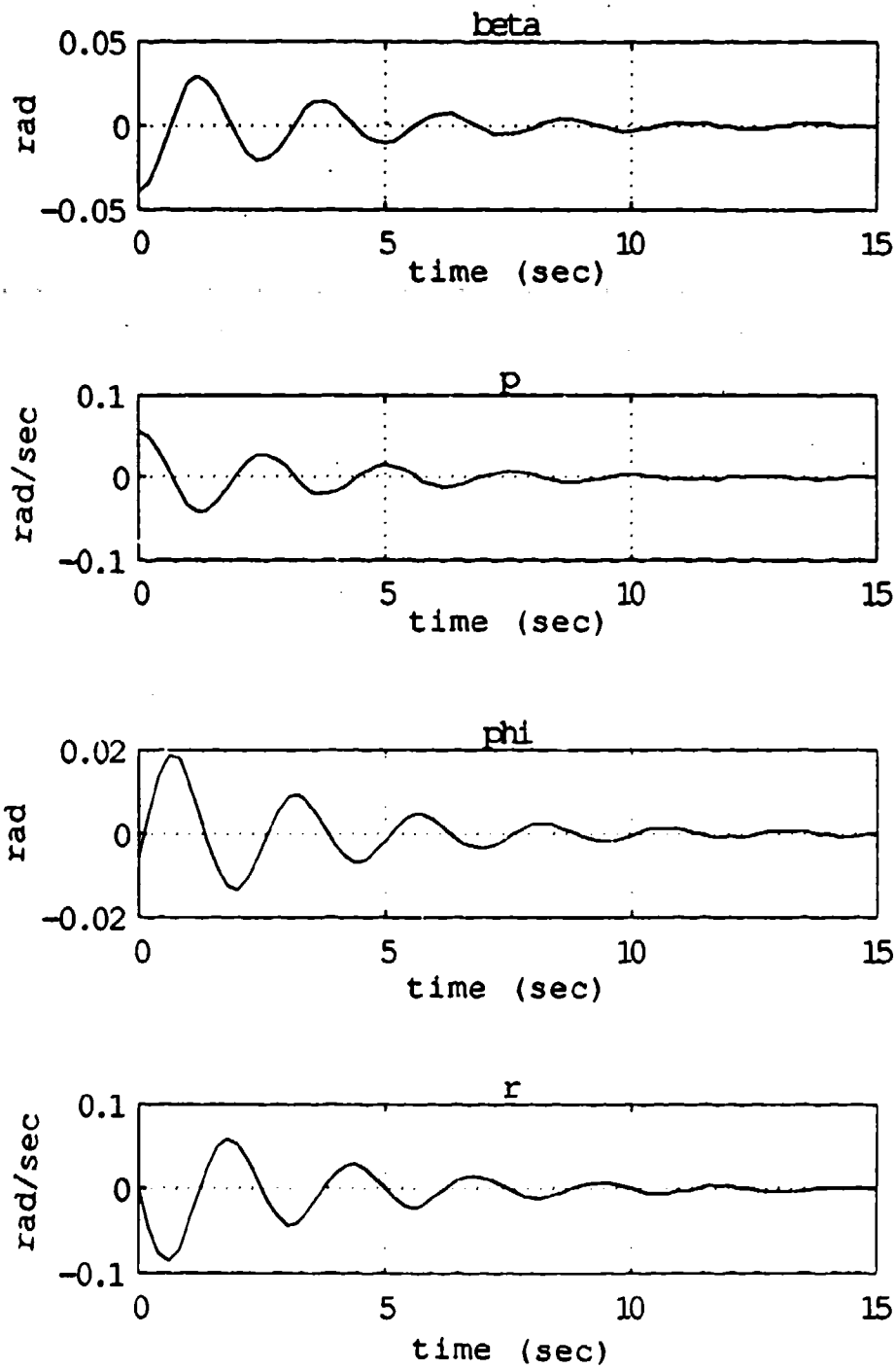

Figure 8. Dutch Roll Response at AOA = 0 degrees

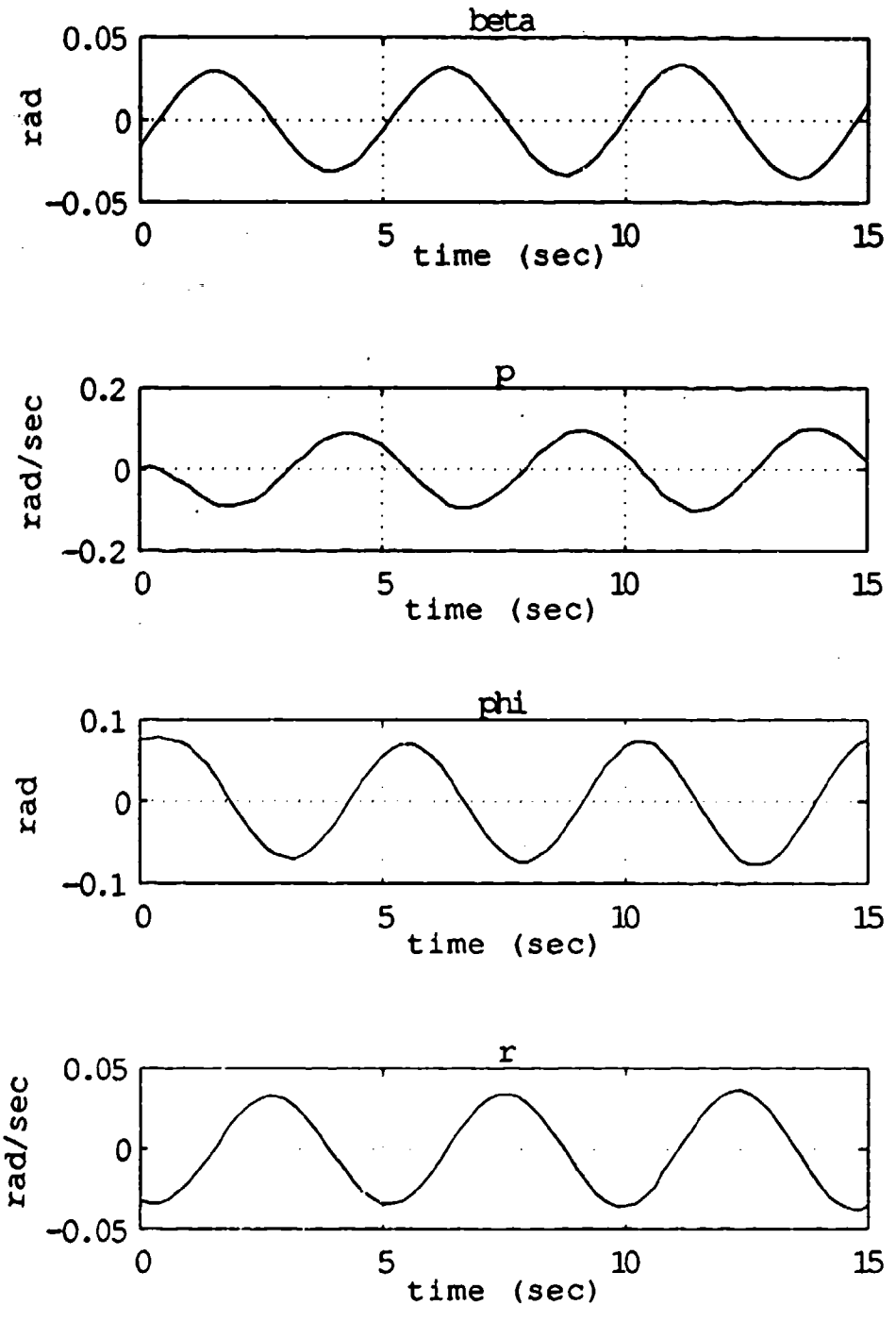

Figure 9. Dutch Roll Response at AOA = 10 degrees

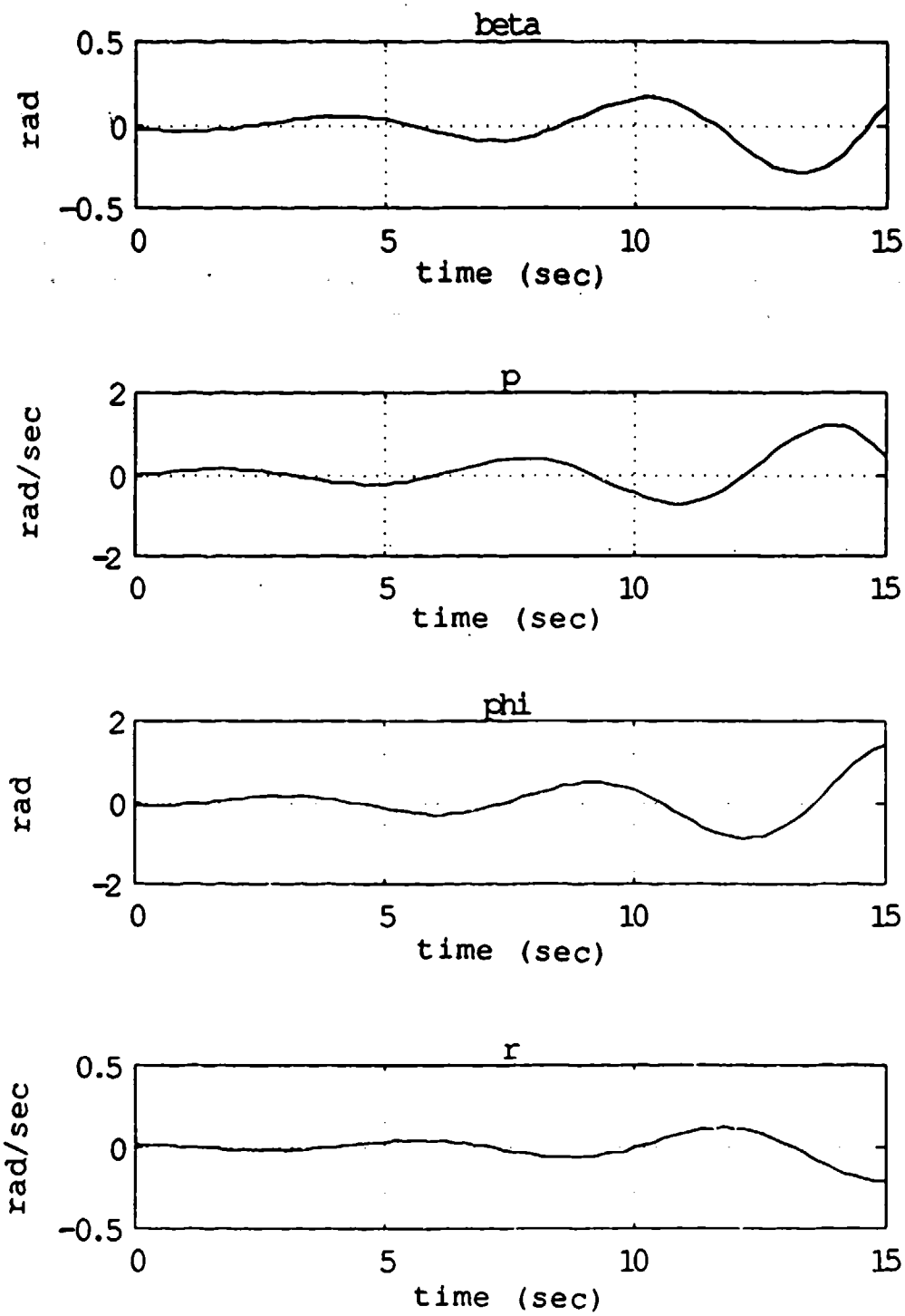

Figure 10. Dutch Roll Response for AOA = 15 degrees

The initial conditions for all of the dutch roll responses used a one-tenth scaling of the normalized complex eigenvector, just as in the short period case.

b. Root locus

An explanation for the behavior of the dutch roll mode is clear when an examination of the placement of the roots in the complex plane is made. A root locus is shown below in Figure 11 for the lateral-directional system's dutch roll roots. Notice the migration of the characteristic roots through the imaginary axis as the angle of attack approaches ten degrees. Once the roots migrate to the right hand half plane, the response changes from a convergent to a divergent oscillation.

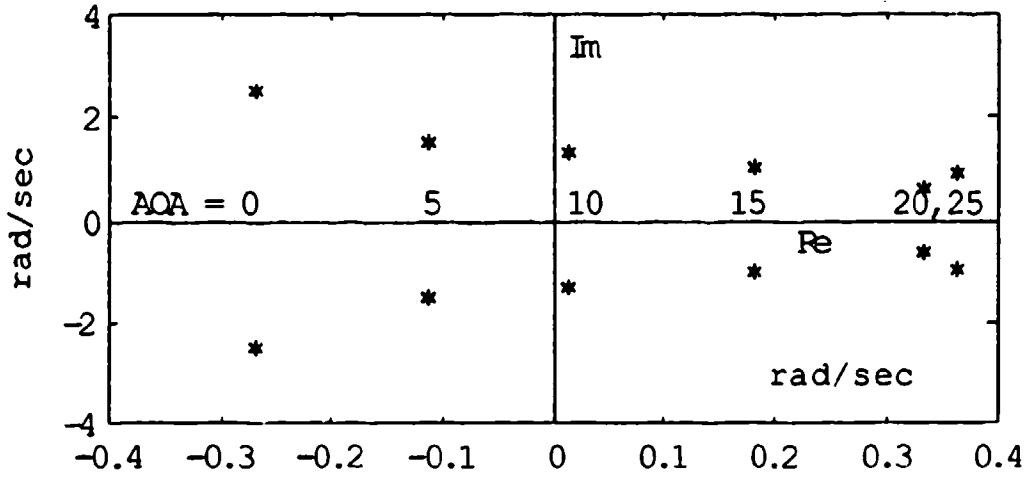

Figure 11. Dutch Roll Root Locus

As previously stated, the instability of the dutch roll mode at high angle of attack results primarily from changes in Cnβ, Clβ and Clp. The root locus plots in Figures 12, 13 and 14 show the sensitivity of the roll, spiral and

dutch roll roots to individual changes in each of these parameters. The direction of root migration shown corresponds to variation of the stability parameter from the value at AOA=0 to AOA=25. All other parameters correspond to AOA=25 values. When the changes in Cnβ, Clβ and Clp occur simultaneously as AOA increases, the individual effects combine to produce a rapid onset of dutch roll instability as shown previously in Figure 11. It was noted that had the values of Cnβ, Clβ and Clp corresponding to zero AOA been held constant as AOA increased, the dutch roll roots would have been stable.

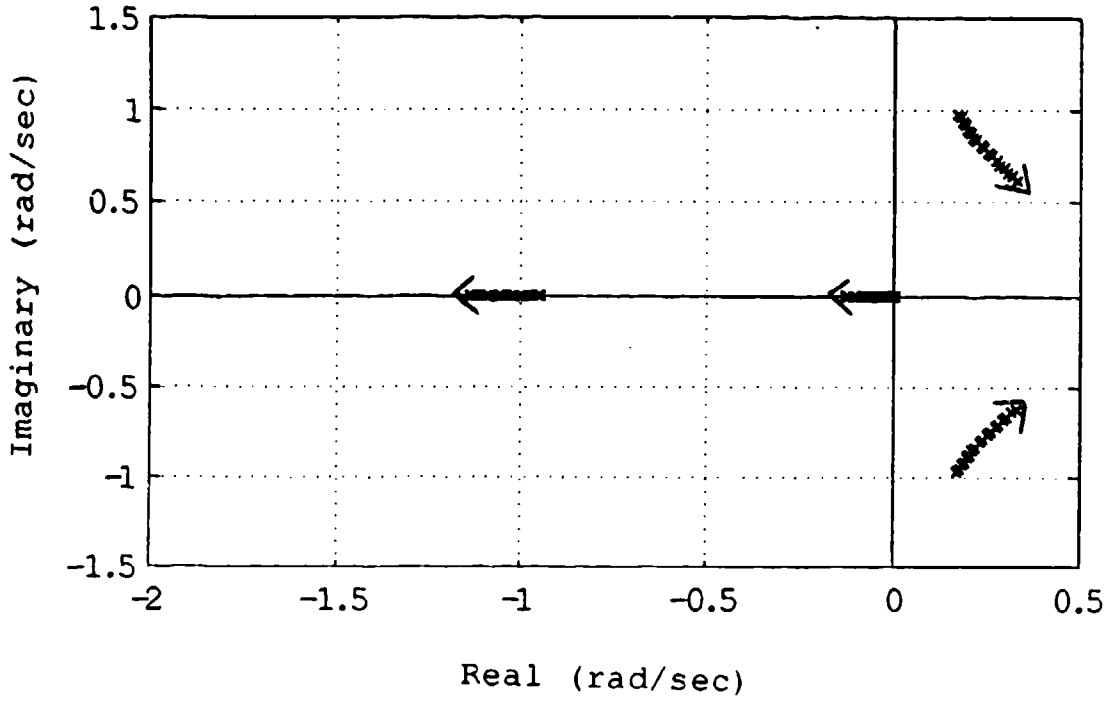

Figure 12. Root Locus for $C_{n\beta}$ Variation

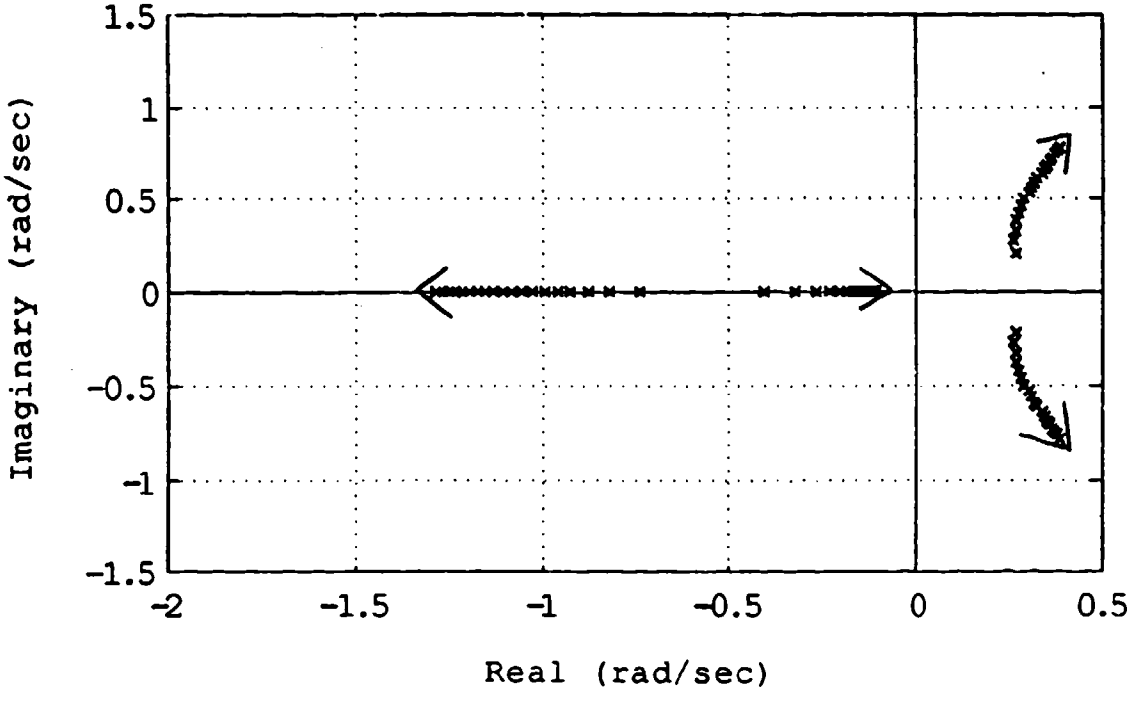

Figure 13. Root Locus for $C_{l\beta}$ Variation

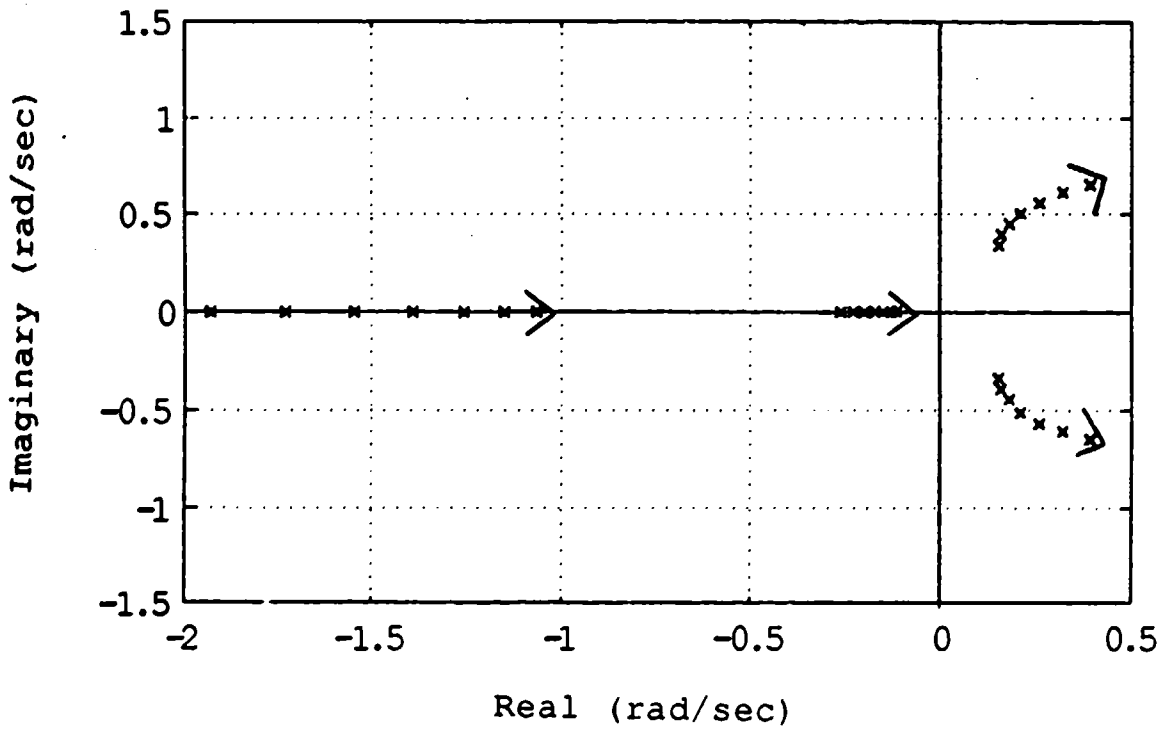

Figure 14. Root Locus for C_{lp} Variation

B. NON-LINEAR ANALYSIS

Now that an understanding of the effect of angle of attack on the linearized system dynamics has been gained, a comprehensive study of the nonlinearized system dynamics is in order. This begins by selecting the coupling option in the computer program, which has the effect of including the nonlinear terms in the equations of motion before numerical integration takes place. Additionally, initial conditions are chosen to demonstrate the effect of coupling from the lateral-directional system to the longitudinal system. Specifically, the lateral-directional initial conditions are the now familiar scaled eigenvector components, while the longitudinal initial conditions are set to zero.

At the low angles of attack where both linear modes are convergent, stable oscillations, one would expect that coupling of the two systems of equations would also produce a convergent, stable solution. This was exactly the case and is clearly evident from examination of Figure 15, the nonlinear response at zero degrees angle of attack. The changes in the lateral-directional parameters from the linear dutch roll response were imperceptible at this angle of attack. The effect of coupling on the longitudinal parameters is also evident from the plots, although the maximum amplitude of the longitudinal perturbations is on the order of a tenth of a degree. Although the longitudinal response shown here is imperceptible from a pilot's point of view, there is some significance to one feature which continues to appear at higher angles of attack. This is the frequency relationship between the roll angle response and the angle of attack response. In every case, the angle of attack perturbations occurred at twice the frequency of the roll response. This is somewhat intuitive, as angle of attack

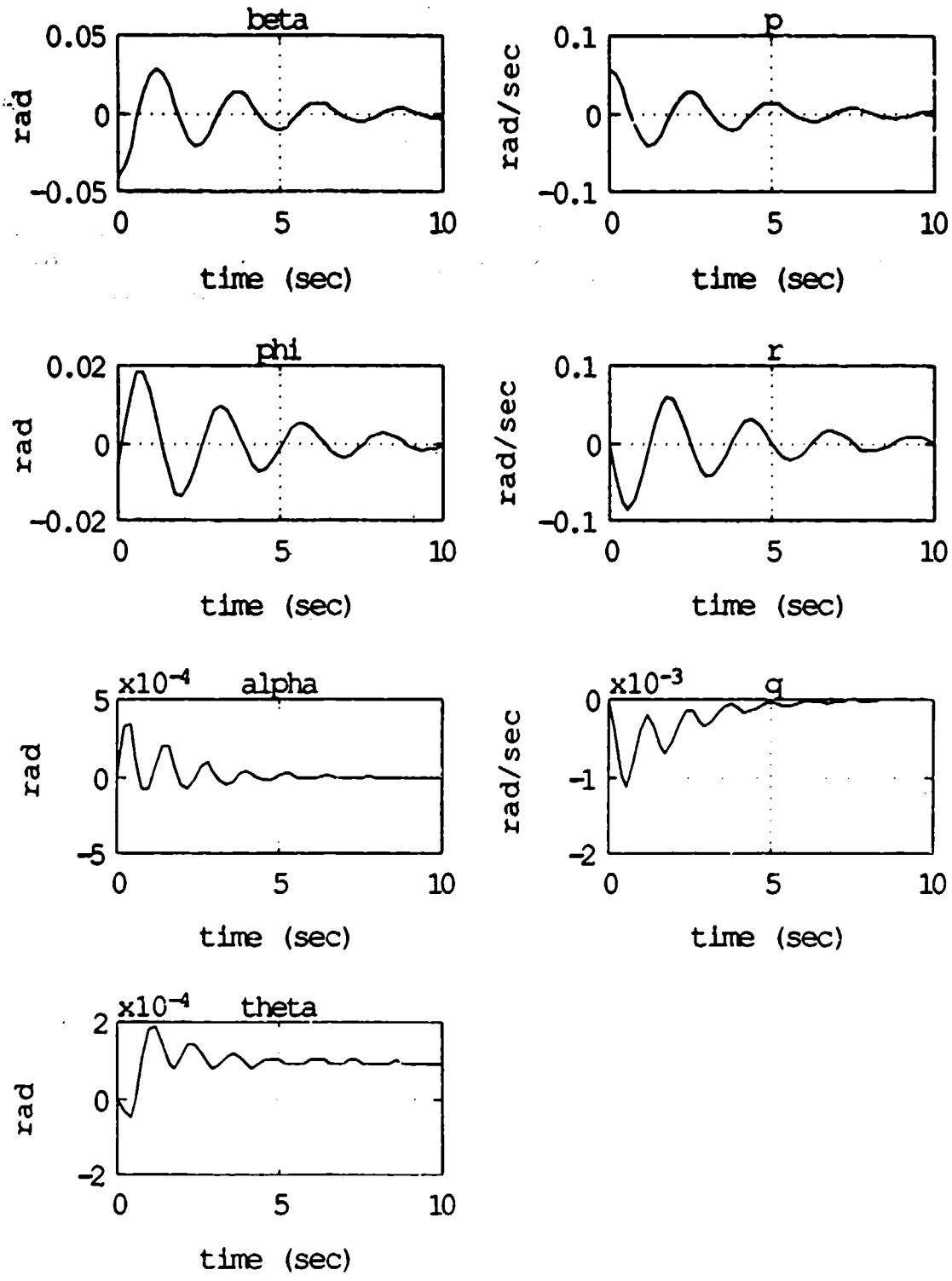

Figure 15. Coupled Response at AOA = 0 degrees

perturbations can be expected to occur with either right or left wing movement. This tendency has been observed in the actual flight test time history traces discussed earlier.

A similar response was obtained for five degrees AOA. Once again, the nonlinear coupling produced very little change from the linear dutch roll response and extremely small longitudinal perturbations. At ten degrees AOA, however, the nonlinear response failed to converge. Instead, a stable, constant magnitude oscillation developed in the lateral-directional parameters which is characteristic of a mild wing rock motion.. This response is shown in Figure 16. The maximum amplitudes of the longitudinal parameters due to the coupling are increasing, but are still insignificant in comparison to the overall response. Note that the mean value of the longitudinal perturbations in angle of attack and pitch rate are displaced from their respective equilibrium positions, while the pitch angle begins to fall off in an oscillatory manner. The presence of limit cycle behavior is clearly shown in this figure.

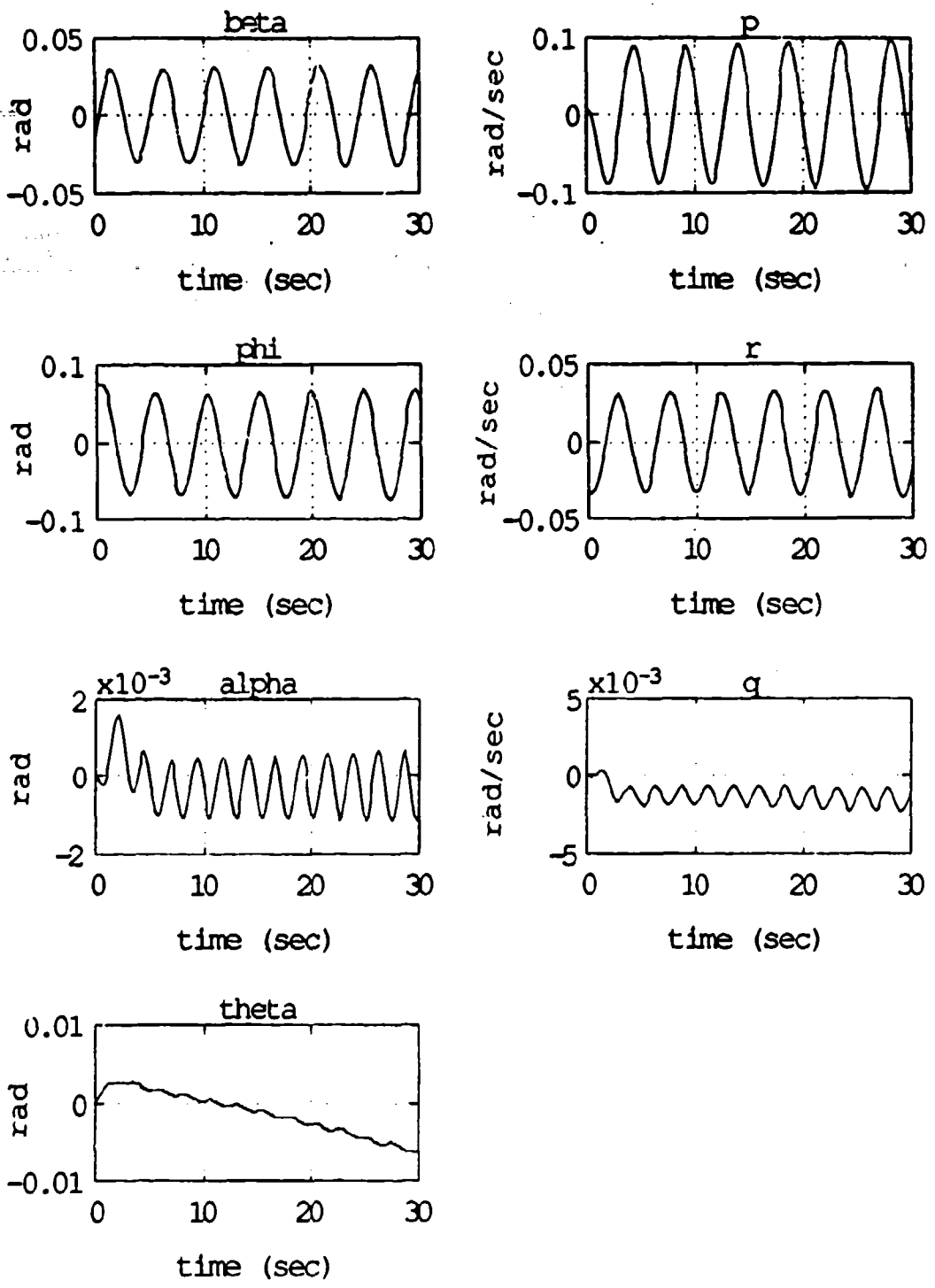

Figure 16. Coupled Response at AOA = 10 degrees

Beyond ten degrees angle of attack, the coupling continued to produce oscillations in the lateral-directional parameters which were indicative of wing rock, while more dramatic changes began to appear in the longitudinal parameters. Responses for AOA=15, 20 and 25 degrees are shown on the following pages in Figures 17 through 19.

The results of this portion of the analysis further demonstrated the development of wing rock limit cycles as a result of nonlinear coupling at high angle of attack. Although the maximum amplitudes for the roll angle and sideslip were somewhat higher than those given in NATOPS for the maneuver flap configuration, the magnitudes were not unreasonable considering the approximations made to obtain the results.

A few other important observations can be made by referring back to the plots of sideslip, roll angle, angle of attack and pitch angle for AOA=20, which have been enlarged in Figures 20a and 20b to show greater detail. The nonlinearity of the sideslip response near the maximum amplitude limits of the oscillation can be seen in Figure 20a. Instead of obtaining the smooth sinusoidal response normally associated with an underdamped system, this response illustrates that the coupling distorts the oscillation. Second, it is noted that as the perturbations in sideslip and roll angle begin, the frequency of the oscillations is very close to the dutch roll frequency. As the coupling takes effect and the limit cycle is established, the frequency of oscillation decreases by approximately 30 percent. This trait was observed at all AOA's where a limit cycle was established and can be attributed to the nonlinear interaction of the longitudinal and lateral-directional modes. For the aircraft modeled in Ref. 4 which displayed a very mild dutch roll instability, this phenomenon was not observed. In that study, the

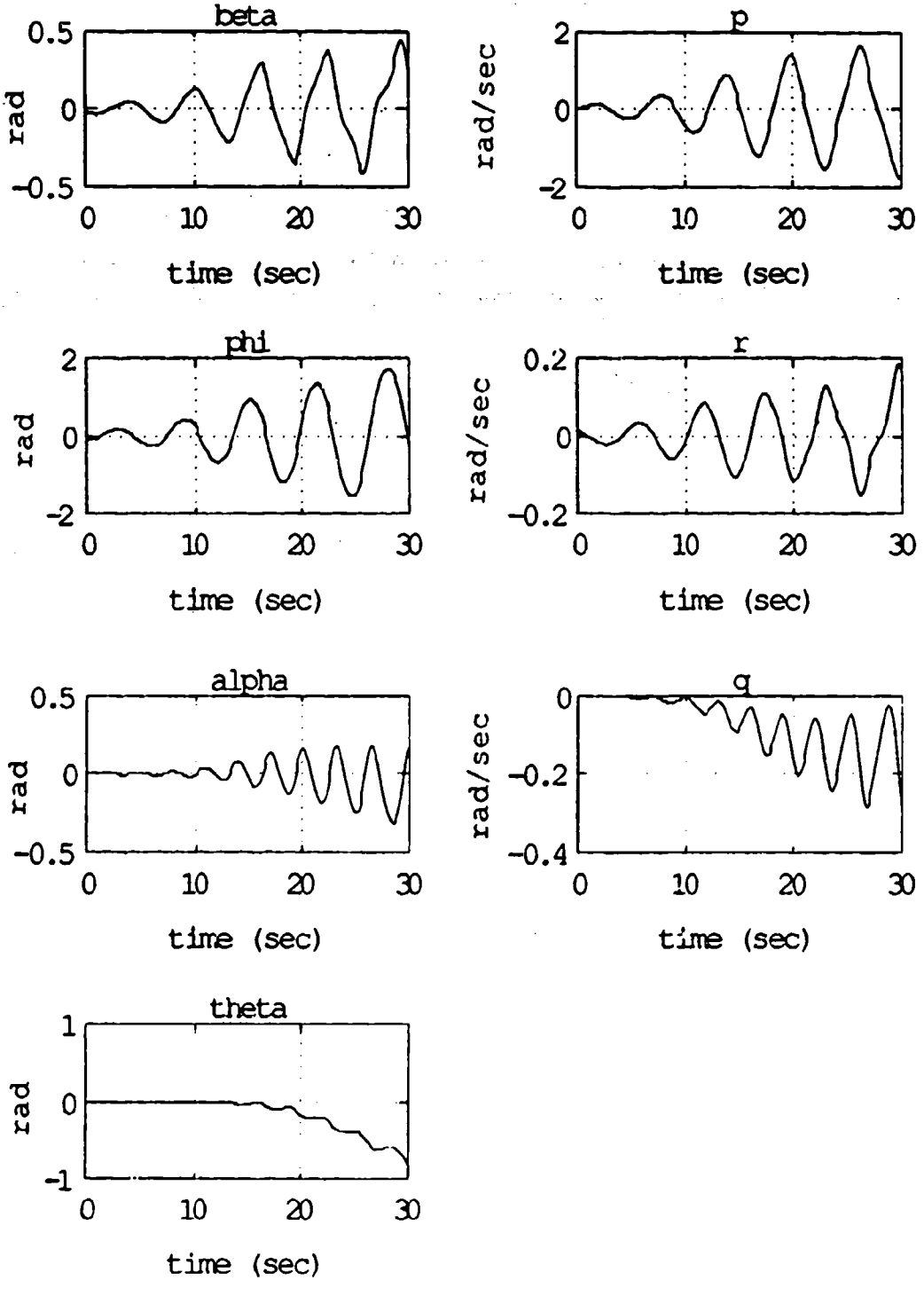

Figure 17. Coupled Response at AOA = 15 degrees

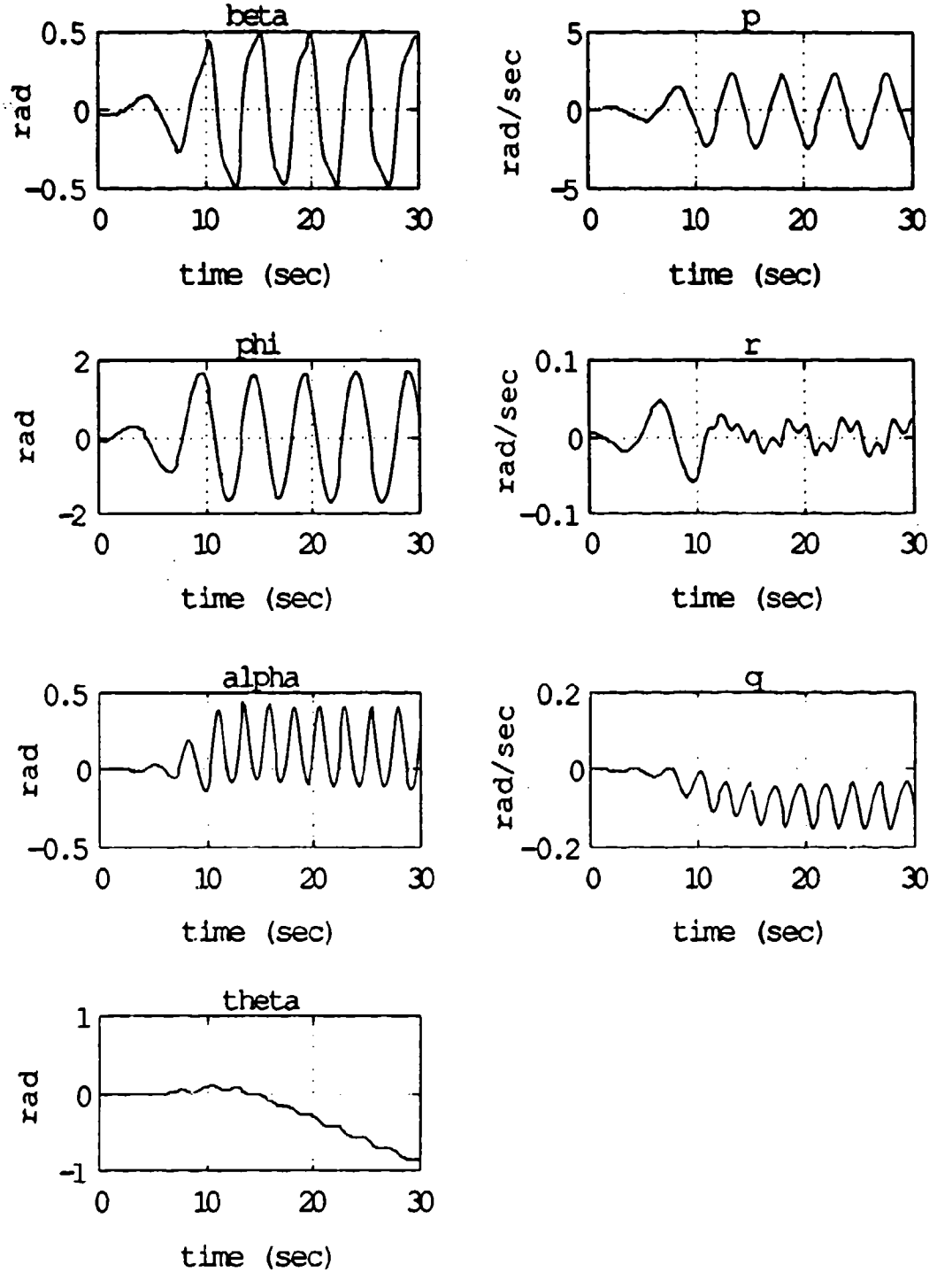

Figure 18. Coupled Response at AOA = 20 degrees

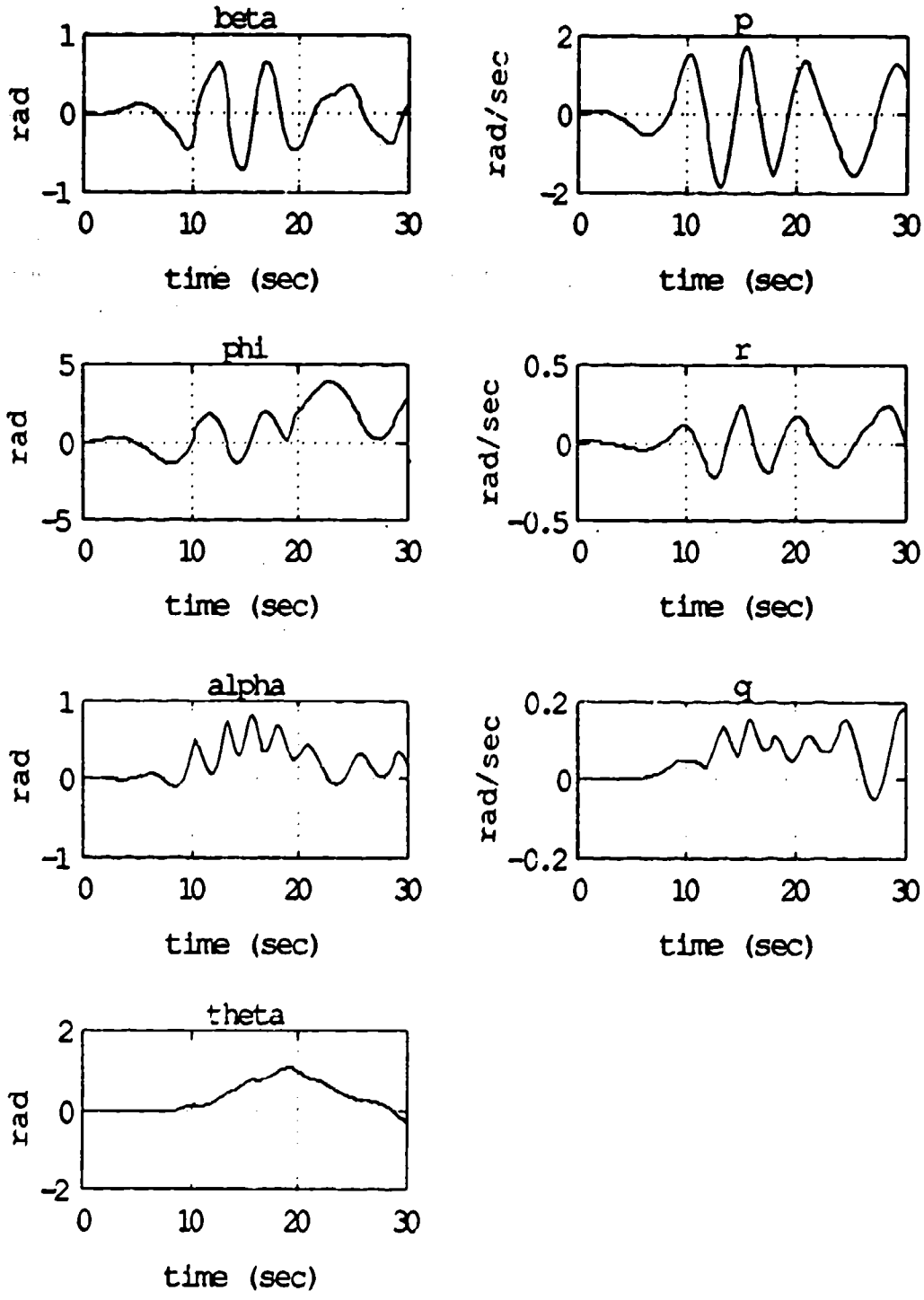

Figure 19. Coupled Response at AOA = 25 degrees

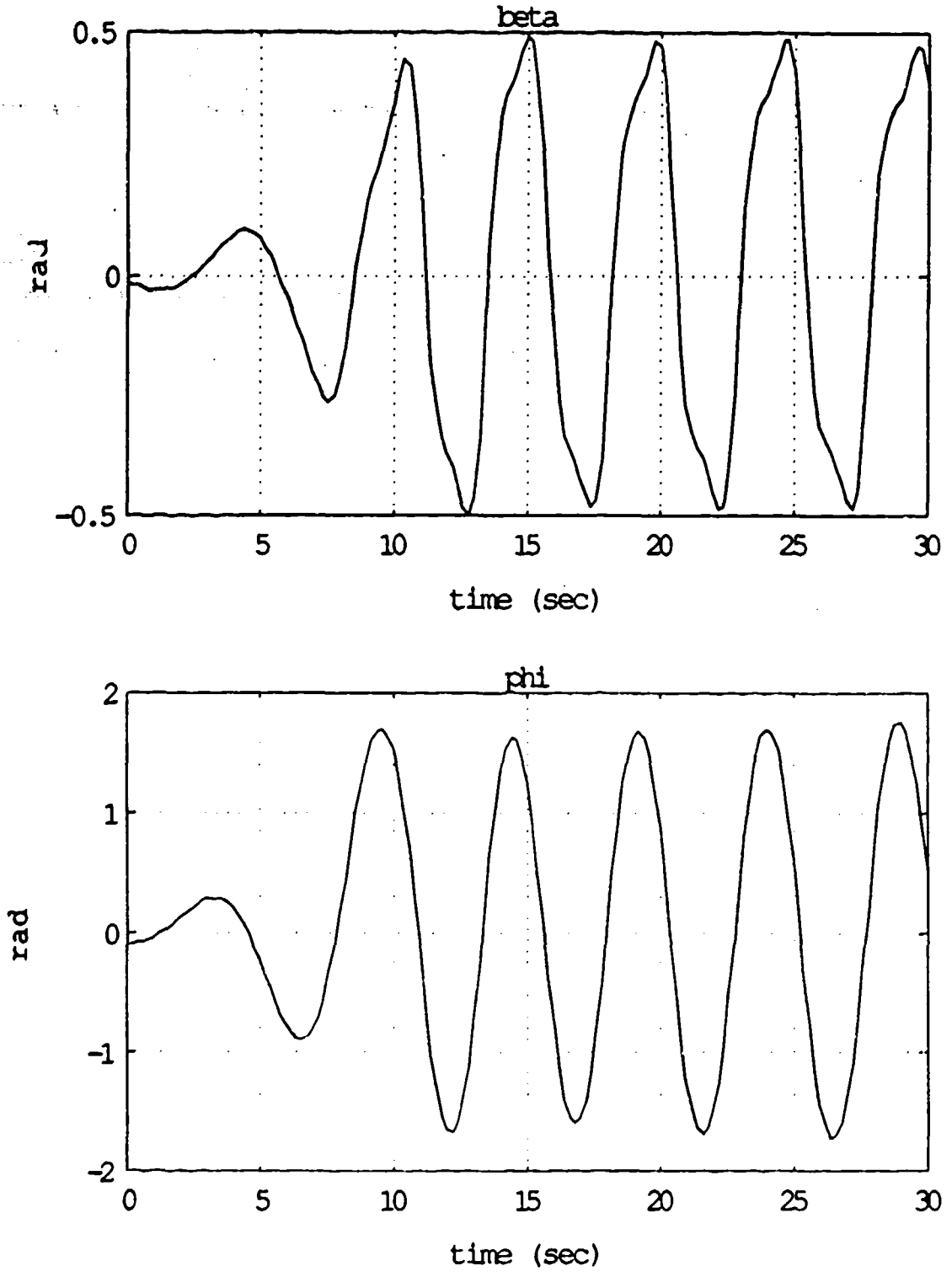

Figure 20a. Detailed View of Coupled Response at AOA = 20 degrees

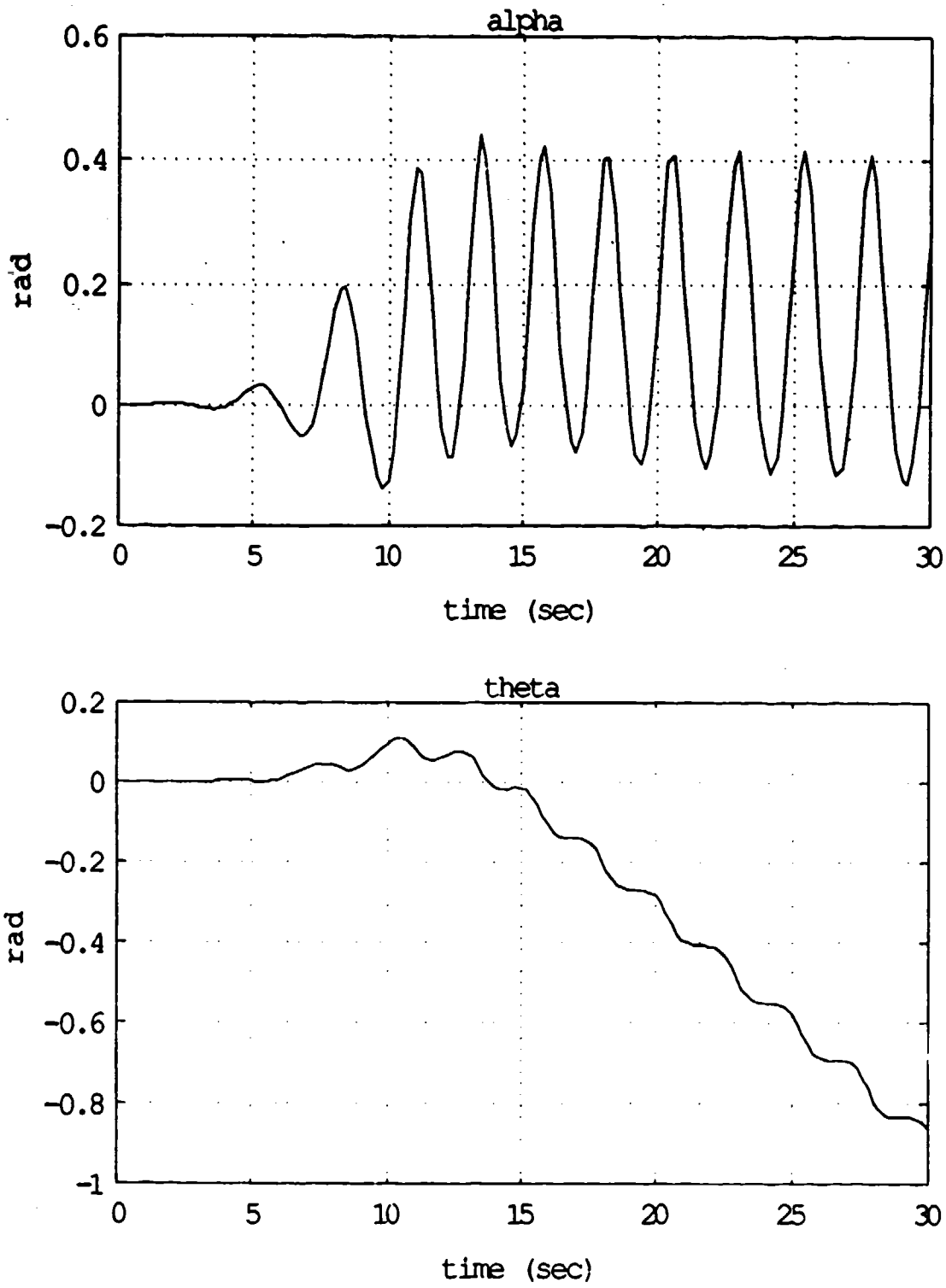

Figure 20b. Detailed View of Coupled Response at AOA = 20 degrees

frequencies of the natural modes were artificially controlled to maintain a harmonic relationship between the short period and the dutch roll response. Here, no such relationship exists. Further study may uncover the dependency of the limit cycle frequency on the characteristic frequencies of the natural modes.

Finally, it was noted that as the limit cycle was established, the mean value of the angle of attack perturbation increased to a value which was slightly higher than its equilibrium position and the pitch angle began to drop. This tendency was also observed in the flight test results. Although the reasons for this are complex as a result of multiple dependency between the perturbation quantities in the fully coupled nonlinear equations, one aspect of the wing rock motion may provide a clue as to its origin. Consider the lift equilibrium during the wing rock motion. The vertical component of lift at any time is proportional to the cosine of the roll angle, which changes continuously with time. Therefore, the average value of lift during one limit cycle oscillation is dependent upon the maximum amplitude of the wing rock and will always be lower than the equilibrium value of lift. As a result of the drop in the average lift per cycle, the aircraft starts to travel on a curvelinear flight path. This response shows up as a loss in altitude. Additionally, the dependence of the nonlinear terms in the angle of attack and pitch angle equations ((15) and (17)) upon the average value of lift is readily apparent by the presence of the $\cos(\phi)$ term. This dependency may be the dominant feature which causes this type of response.

VII. RESULTS

The convergent nature of the linearized short period response and the divergent nature of the linearized dutch roll response for the same flight condition indicated that the numerical procedure used produced time history traces consistent with the behavior of stable and unstable linear systems, respectively.

When the equations were modified to include the nonlinear terms, the responses for the low angles of attack (AOA=0 and 5 degrees) did not change appreciably, although the influence of the coupling was apparent in small longitudinal perturbations. At these angles of attack, both the longitudinal and lateral-directional characteristic roots were stable, resulting in an asymptotically stable solution in the sense of Liapunov [Ref. 14]. It has been demonstrated that although coupling between the two sets of equations occurred, the overall result failed to produce a limit cycle response.

When the nonlinear equations were analyzed at the higher angles of attack, however, the presence of unstable dutch roll eigenvalues destroyed the asymptotic stability. Even so, the coupling between the longitudinal and lateral-directional equations still yielded a stable system response in the form of a wing rock limit cycle oscillation.

VIII. CONCLUSIONS

A numerical analysis of the nonlinear equations of motion has been conducted to investigate the contribution of inertial coupling to the development of wing rock in the F-14 aircraft. Actual wind tunnel data was used to develop all of the stability parameters for the analysis. Although a number of simplifying assumptions were made, the analysis indicated that inertial coupling of a stable short period mode and an unstable dutch roll mode can result in a response very much like that encountered in the aircraft, especially for the lateral-directional parameters. The trends displayed in the longitudinal parameters as a result of the coupling were consistent with flight tests; however, the magnitude of the excursions from the trim position for these parameters was greater than expected. Although these deviations appeared to be beyond reason, the results obtained here should not be discounted on this basis. The intention was to conduct a preliminary investigation into the mechanics of wing rock for the F-14 in hopes of uncovering a relatively simple explanation for the aircraft's behavior. In the pursuit of this goal, it has been demonstrated that a stable short period mode can feed damping energy into an unstable dutch roll mode to produce a bounded wing rock type oscillation. Unquestionably there is a great deal of further research which must be done to fully understand the motion, including more detailed analyses which disregard some of the simplifications made in this analysis and which promise to yield results which are more consistent with the aircraft's actual response. The following section highlights a few of these techniques.

IX. RECOMMENDATIONS FOR FURTHER RESEARCH

The analysis presented here is only a start. It serves to illustrate that numerical techniques can be used to solve the nonlinear equations of motion and to predict the response of aircraft subject to specified initial conditions. There exists a wide variety of related research topics that can further our understanding of nonlinear flight mechanics. Some of these topics are addressed in the paragraphs which follow.

A. EIGHT DEGREE OF FREEDOM ANALYSIS

Perhaps the least difficult of all suggestions to follow for continued research in this field would be the extension of the analysis to eight degrees of freedom. The eighth parameter of interest, perturbation velocity, was held constant during this analysis based on an approximation of constant velocity during the wing rock motion. To bring the analysis to eight degrees of freedom, the X-force equation would be introduced in its full non-linear form, the pertinent stability parameters obtained from further analysis of the available data base and the computer code modified. The influence of the additional degree of freedom on both the linearized analysis of the longitudinal parameters and the full non-linear analysis would warrant a full investigation of the changes in the dynamic response, especially given the tendency of the aircraft to end up in a nose down attitude where changes in velocity are sure to occur.

B. TIME DEPENDENT STABILITY PARAMETER ANALYSIS

A much more difficult undertaking would involve the incorporation of time dependent stability parameters into the analysis. As stated previously, the data base contains an extensive list of stability parameters as a function of multiple variables; however, only derivative values corresponding to the steady, level flight trim condition were used for this investigation. Recall that as the aircraft moves, the pitch, roll and yaw rates developed contribute to the stability of the aircraft and may play a significant role in the overall response of the aircraft. Furthermore, changes in AOA and sideslip angle as the aircraft moves about its equilibrium position also affect the stability parameters. Lastly, although this analysis was conducted controls fixed, on the actual aircraft, control surface position also influences the stability of the aircraft. Therefore, although this analysis proceeded under the approximation of constant stability characteristics as part of a planned buildup to a more detailed analysis, it nevertheless neglects the changing dynamic behavior of the aircraft as it translates and rotates. Ease of implementation for the first attempt at numerical creation of the wing rock motion from wind tunnel data was also a factor in choosing this approximation. Although this simplification may be appropriate for some aircraft operating at relatively low AOA, it may be the reason for obtaining such large perturbations in the longitudinal parameters at high AOA.

In order to implement such a change in the analysis, one of several options must be exercised to allow for variable stability parameters. One option might involve the development of subroutines which would allow the computer to conduct a table look up of dimensionless stability parameters and subsequent

conversion into dimensional form. This would require the availability of the entire data base to the code, as well as restructuring of the code to accommodate the table look up feature.

Another option might involve the use of multi-variable curve fitting to obtain very accurate approximations of the dimensionless stability parameters as the aircraft moves.

C. OPTIMIZATION OF NUMERICAL SOLUTION

Still another possibility for future research in this area involves numerical optimization. Numerical techniques commonly used to obtain solutions for systems of differential equations vary widely in their accuracy and suitability for a given problem. The "exactness" of a numerical solution is very much dependent upon the methods used to numerically approximate the equations, the desired accuracy of the solution and the acceptable numerical cost in determining that solution. Similarly, the stability of a numerical procedure is also quite important in that it determines the acceptable variation of parameters, such as the time increment, which force a convergent solution. Care must be taken when conducting numerical analysis to account for the stability characteristics and desired accuracy of the solution. Therefore, a study attempting to optimize the numerical technique used to obtain the time history data points may be in order. For example, a number of different finite difference schemes could be used to obtain and compare solutions, computation time, overall efficiency, etc.

D. INCORPORATION OF ACTUAL FLIGHT TEST RESULTS

Once a numerical technique is developed to more accurately and efficiently model all aspects of the wing rock motion, the incorporation of additional flight

test results from an instrumented aircraft could be used to verify results obtained from the study. By utilizing the same initial conditions, aircraft configuration, geometry and inertia characteristics as inputs into a similar analysis, it would be possible to try to numerically reconstruct the true response of the aircraft.

E. NUMERICAL ANALYSIS OF F/A-18 WING ROCK

In that a complete F/A-18 flight simulation program and data base are available for research use, a similar analysis conducted on that aircraft may provide some clues as to the mechanics behind F/A-18 wing rock. It is known that the aircraft displays a complex wing rock motion at very high AOA which cannot be damped out by pilot input, flight control computer or any combination of the two. The data base can be obtained from the NASA Ames Research Center/Dryden Flight Research Facility located at Edwards AFB, CA.

APPENDIX A.- DATA BASE MANIPULATION

The stability derivatives needed to conduct this analysis were extracted from tabular wind tunnel data provided by the Grumman Corporation [Ref. 9]. This appendix is provided to give the reader some insight as to how the tabular data was used to extract the necessary information for the study.

The first things needed to conduct the analysis at any particular angle of attack were the velocity, thrust required and control surface positions for steady, level flight (SLF) at that AOA. Assumptions of perfect lateral symmetry about the X-Z plane and the absence of gyroscopic effects led to the assignment of zero deflection for any lateral or directional control surfaces. The trim velocity and stabilator position were found by simultaneously solving the following two equations for alpha and δs (stabilator position) in an iterative process:

$$C_{m_{cg}} = C_{m_0} + C_{m_{thrust}} + C_{m_\alpha}\alpha + C_{m_{\delta s}}\delta s \qquad (23)$$

$$C_L = C_{L_0} + C_{L_{thrust}} + C_{L_\alpha}\alpha + C_{L_{\delta s}}\delta s \qquad (24)$$

Specifically, the desired trim AOA was designated and a guess at the appropriate trim velocity was made. C_{mcg} is zero in SLF and C_L can be calculated easily by using the assumed trim velocity and the weight of the aircraft. Values for C_{m0}, $C_{m\alpha}$, C_{Lo}, and $C_{L\alpha}$ were obtained by constructing crossplots of the data given in the tables to get the appropriate slope. Local derivatives were used in all cases where the data was nonlinear. $C_{m\delta s}$ was taken

directly from the tables and $C_{L\delta s}$ was obtained by doing a coordinate transformation through the angle of attack of $C_{x\delta s}$ and $C_{z\delta s}$ data in the table. In order to find $C_{Lthrust}$ and $C_{mthrust}$, the thrust required for SLF had to be determined by finding the drag in SLF at the desired AOA. This was accomplished by doing another coordinate transformation on the C_{x0}, C_{z0}, $C_{x\delta s}$ and $C_{z\delta s}$ information in the table. A plot of C_D vs alpha was constructed from this data for each different stabilator setting given in the tables. From this plot, an estimate of the drag could be determined. This plot is shown below in Figure 21.

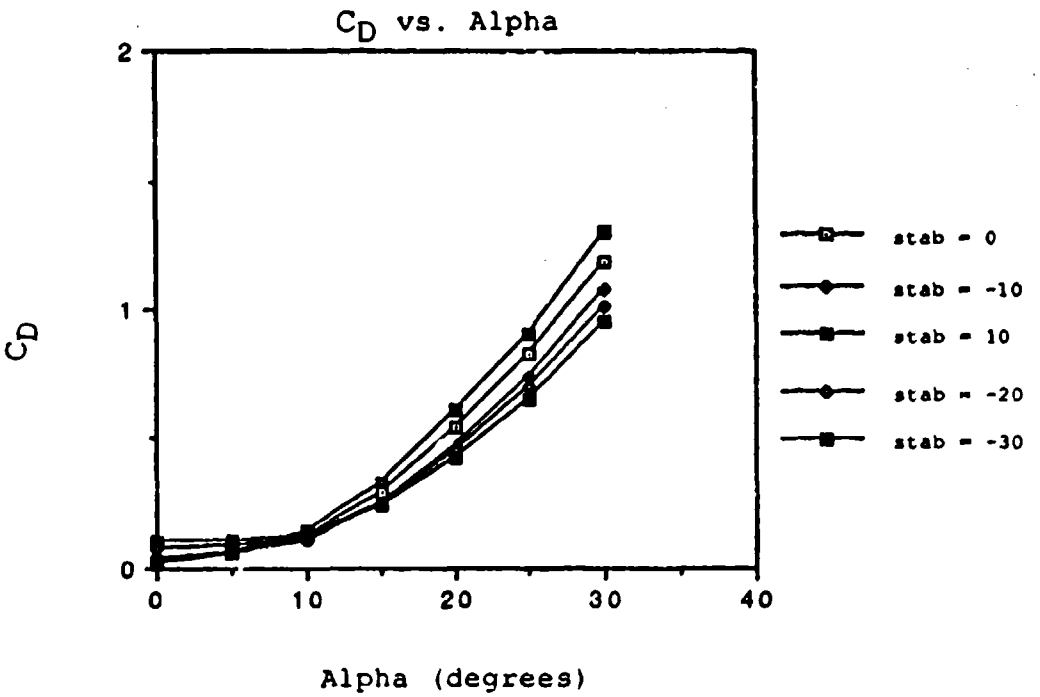

Figure 21. C_D vs Alpha

With an estimate of the drag, thrust required is immediately known. This is converted into a pitching moment contribution and a lift contribution, which are then converted into their final coefficient form. With all of the parameters for these two equations known, the equations are solved for alpha and δs. The initial assumed trim velocity is iterated until a match is made between the calculated AOA and the desired AOA. When a match is made, the stabilator setting calculated is used to update the determination of drag. The equations are solved again with this new drag figure and after only a few iterations, the calculation converges on the final result for stabilator setting.

A convenient cross check for this procedure is available by building up a plot of C_{mcg} vs. alpha by combining C_{m0}, $C_{m\delta s}$ and $C_{mthrust}$ information. This procedure results in the plot shown below in Figure 22. This plot can be used to determine the stabilator setting required to maintain $C_{mcg} = 0$ (i.e., SLF) at any desired AOA.

The determination of stabilator setting is important because some of the data in the tables is dependent on this parameter. Once this setting is known, all of the stability derivatives can be found. The following steps contain a brief description of the remaining procedures to obtain these derivatives.

1) $C_{y\beta}$, $C_{n\beta}$, $C_{l\beta}$ and $C_{z\alpha}$ are found by constructing crossplots of the data given in the tables and taking local derivatives.
2) C_{yp}, C_{yr}, C_{lp}, C_{lr}, C_{np}, C_{nr} and C_{mq} are taken directly from the tables.
3) C_{Lq} is found by doing a coordinate transformation of C_{xq} and C_{zq}.

All of these dimensionless coefficients are then converted into dimensional form using standard conversion formulas. At this point, the derivatives are ready to be used in the analysis.

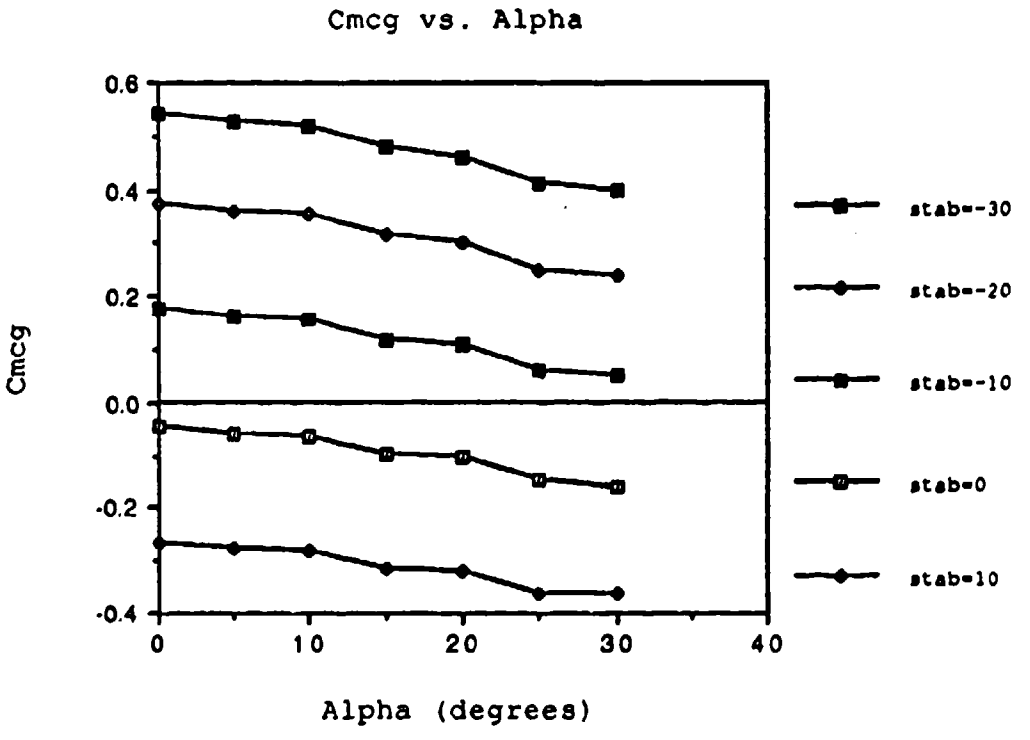

Figure 22. C_{mcg} vs Alpha

APPENDIX B.- COMPUTER PROGRAM

```
100 REM F14 WING ROCK PROGRAM
110 REM DATA FOR THE F14 AT AOA=20 DEGREES, Vtrim=213 fps
120 REM A( , ) = PLANT MATRIX
130 REM XK( ) = PERTURBATION QUANTITY (PQ)
140 REM XK1( ) = ESTIMATION OF PQ AT NEXT FULL TIME STEP BASED
150 REM          ON DERIVATIVE AT CURRENT TIME STEP
160 REM XK15( ) = ESTIMATION OF PQ AT HALF TIME STEP BASED ON
170 REM           DERIVATIVE AT CURRENT TIME STEP
180 REM XK2( ) = ESTIMATION OF PQ AT FULL TIME STEP BASED ON
190 REM          DERIVATIVE AT HALF TIME STEP
200 REM XSUM( ) =  DERIVATIVE AT HALF OR FULL TIME STEP
210 REM NL( ) = NONLINEAR DERIVATIVE TERMS
220 REM XKMAX( ) = MAX VALUE OF PQ

300 DIM  A(10,10),XK(10),XK1(10),XK15(10),XK2(10)
310 DIM  XSUM(10),NL(10),XKMAX(10)
320  ALPHA=20
330  VTRIM=213
340   PI=3.1415927#
350  U=VTRIM*COS(ALPHA*PI/180)
360 REM DEFINE INERTIAL PROPERTIES
370  AIX=51509!:AIY=232773!:AIZ=275627!:AIXZ=2654
380 REM DEFINE TERMS IN EQNS OF MOTION
390  AIQRL=(AIY-AIZ)/AIX : AIPQN=  (AIX-AIY)/AIZ
400  AIRPM=(AIZ-AIX)/AIY
410 AIPBM = -.16 : AZADOT=0 :THET0 =ALPHA*PI/180
420 REM AIPBM is Malphadot, AZADOT=Zalphadot
430 GU = 32.17/U
440 DT=.05 : DT2=.5*DT

500 REM DATA FOR PLANTS.  ROWS 1-4 LAT-DIR, ROWS 5-7 LONG
510 DATA  -.0491,.0035,.1511,-1.0007,0,0,0
520 DATA  -6.338,-.5290,0,.6877,0,0,0
```

```
530 DATA  0,1,0,0,0,0,0
540 DATA  -.0515,-.0692,0,-.1186,0,0,0
550 DATA  0,0,0,0,-.2671,.9659,-.0550
560 DATA  0,0,0,0,-.2285,-.5278,.0088
570 DATA  0,0,0,0,0,1,0
580 REM READ IN PLANT DATA TO MATRIX A( )
590 FOR I=1 TO 7
600    FOR J=1 TO 7
610    READ A(I,J)
620    NEXT J
630 NEXT I

700 REM INITIALIZE MATRICES FOR COMPUTATION
710 FOR I=1 TO 7
720 XK(I)=0 : XK1(I)=0 : XK15(I)=O : XK2(I)=0
730 NEXT I

800 REM DEFINE 1/10th SCALE DR EIGENVECTOR IC'S
810 XK(1)= -.01434: XK(2)=0: XK(3)=-.09212   : XK(4)=.0055
820 REM SET SP IC'S TO ZERO
830 XK(5)= 0: XK(6)=0: XK(7)=0

900 REM INPUT "USE INERTIAL COUPLING (Y/N)";A$
910 REM INPUT "CREATE DATA FILES (Y/N)";B$
920 A$="Y" : B$="Y"
930 IF B$="Y" THEN GOSUB 2000
940 REM PRINT INITIAL VALUES OF PQ'S
950 GOSUB 2100

1000 REM PERFORM NUMERICAL INTEGRATION
1010  T=0
1020 FOR K=1 TO 400
1030  T=K*DT

1100    REM CALCULATE DERIVATIVES AT CURRENT TIME STEP
1100    REM USING PQ'S AT CURRENT TIME STEP
1120     FOR I=1 TO 7
1130     XSUM(I)=0
```

```
1140      FOR J=1 TO 7
1150       XSUM(I)=XSUM(I)+A(I,J)*XK(J)
1160      NEXT J

1200    REM CALCULATE ESTIMATED PQ'S AT HALF AND FULL TIME
1210    REM  STEP BASED ON DERIVATIVES AT CURRENT TIME STEP
1220     XK15(I)=XK(I)+DT2*XSUM(I)
1230     XK1(I)=XK(I)+DT*XSUM(I)
1240    NEXT I
1250    REM IF NECESSARY, CALCULATE NONLINEAR TERMS
1260    IF A$="N" THEN GOTO 1420
1270    GOSUB 2200
1280    REM CORRECT XK15( ) & XK1( ) FOR NONLINEAR TERMS
1290    FOR I=1 TO 7
1300     XK15(I)=XK15(I)+DT2*NL(I)
1310     XK1(I)=XK1(I)+DT*NL(I)
1320    NEXT I

1400    REM CALCUALTE DERIVATIVE AT HALF TIME STEP
1410    REM USING ESTIMATED PQ'S AT HALF TIME STEP
1420    FOR I=1 TO 7
1430    XSUM(I)=0
1440      FOR J=1 TO 7
1450       XSUM(I)=XSUM(I)+A(I,J)*XK15(J)
1460      NEXT J

1500    REM CALCULATE ESTIMATED PQ'S AT FULL TIME STEP
1510    REM BASED ON DERIVATIVE AT HALF TIME STEP
1520     XK2(I)=XK15(I)+DT2*XSUM(I)
1530    NEXT I
1540    REM IF NECESSARY, CALCULATE NONLINEAR TERMS
1550    IF A$="N" THEN GOTO 1720
1560    GOSUB 2400
1570    REM CORRECT XK2( ) FOR NONLINEAR TERMS
1580    FOR I= 1 TO 7
1590     XK2(I)=XK2(I)+DT2*NL(I)
1600    NEXT I
```

```
1700   REM APPLY RICHARDSON'S EXTRAPOLATION TO GET
1710   REM FINAL VALUE AT NEW TIME STEP
1720    FOR I=1 TO 7
1730      XK(I)=2*XK2(I)-XK1(I)

1800   REM FIND MAX VALUE OF EACH PQ
1810    IF ABS(XK(I))>XKmax(I) THEN XKmax(I)=ABS(XK(I))

1900    NEXT I
1910   REM PRINT RESULTS
1920    IF (INT(K/4)=(K/4)) THEN GOSUB 2100
1930 NEXT K
1940 IF B$="Y" THEN GOSUB 2700
1950 END

2000 REM S/R FOR OPENING DATA FILES
2010 OPEN "data" FOR OUTPUT AS #1
2020 OPEN "maxdata" FOR OUTPUT AS #2
2030 RETURN

2100 REM  S/R PRINTS TIME AND STATE VECTOR ON SCREEN
2110 REM AND STORES DATA IN FILE FOR SUBSEQUENT PLOTTING
2120  PRINT USING  "###.####";T;XK(1);XK(2);XK(3);XK(4),
!       XK(5),XK(6),XK(7)
2130 IF B$="Y" THEN GOSUB 2600
2140 RETURN

2200 REM S/R FOR FIRST USE OF NON LINEAR TERMS
2210 THETA =THET0+XK(7) : CTHETA=COS(THETA) :
!       TTHETA=TAN(THETA)
2220 PHI=XK(3) : SPHI=SIN(PHI) : CPHI=COS(PHI)
2230  NL(1)=XK(2)*XK(5)+GU*CTHETA*SPHI-A(1,3)*XK(3)
2240  NL(2)=AIQRL*XK(6)*XK(4)
2250  NL(3)=(XK(6)*SPHI+XK(4)*CPHI)*TTHETA
2260  NL(4)=AIPQN*XK(2)*XK(6)
2270  NL(5)=-XK(2)*XK(1)*U/(U-AZADOT)+32.17/(U-AZADOT)
!       *(CTHETA*CPHI-COS(THET0)+SIN(THET0)*XK(7))
2280  NL(6)=AIRPM*XK(4)*XK(2)+AIPBM*NL(5)
```

```
2290  NL(7)=XK(6)*(CPHI-1)-XK(4)*SPHI
2300 RETURN

2400 REM S/R FOR SECOND USE OF NON LINEAR TERMS
2410 THETA =THET0+XK15(7) : CTHETA=COS(THETA) :
!      TTHETA=TAN(THETA)
2420 PHI=XK15(3) : SPHI=SIN(PHI) : CPHI=COS(PHI)
2430  NL(1)=XK15(2)*XK15(5)+GU*CTHETA*SPHI-A(1,3)*XK15(3)
2440  NL(2)=AIQRL*XK15(6)*XK15(4)
2450  NL(3)=(XK15(6)*SPHI+XK15(4)*CPHI)*TTHETA
2460  NL(4)=AIPQN*XK15(2)*XK15(6)
2470  NL(5)=-XK15(2)*XK15(1)*U/(U-AZADOT)+32.17/(U-AZADOT)
!       *(CTHETA*CPHI-COS(THET0)+SIN(THET0)*XK(7))
2480  NL(6)=AIRPM*XK15(4)*XK15(2)+AIPBM*NL(5)
2490  NL(7)=XK15(6)*(CPHI-1)-XK15(4)*SPHI
2500 RETURN

2600 REM S/R FOR STORING DATA TO FILE
2610  PRINT #1, USING  "###.#    +###.#####    +###.#####
2620 REM CONTINUE PRINT USING +###.#####    +###.#####
2630  REM  CONTINUE +###.#####     +###.#####   +###.#####";
2640 REM  CONTINUE T,XK(1),XK(2),XK(3),XK(4),XK(5),XK(6),XK(7)
2650 RETURN

2700 REM S/R TO CLOSE DATA FILE
2710 CLOSE #1
2720  PRINT #2, USING  "+#.##     +###.#####     +###.#####
2730 REM CONTINUE PRINT USING +###.#####";zeta,XKmax(1)
2740 REM CONTINUE ,XKmax(3),XKmax(5)
2750 CLOSE #2
2760 PRINT "DATA FILES CLOSED"
2770 RETURN
```

REFERENCES

1. Journal of Aircraft, Vol. 16, No. 3, Report 79-4037, *Wing Rock Due to Aerodynamic Hysteresis*, Schmidt, L.V., pp. 129-133, March 1979.

2. Journal of Aircraft, Vol. 9, No. 9, Report 72-62, *Investigation of Nonlinear Motion Experienced on a Slender-Wing Research Aircraft*, Ross, A.J., pp. 625-631, September, 1972.

3. Journal of Aircraft, Vol. 26, No. 1, Report 87-2496, *Analytic Prediction of the Maximum Amplitude of Slender Wing Rock*, Ericsson, L.E., pp. 35-39, January, 1989.

4. Schmidt, L.V. and Wright, S.R., "Wing Rock Due to Inertial Coupling," paper submitted to AIAA Atmospheric Flight Mechanics Conference to be held in New Orleans, Louisiana, June 1991.

5. AIAA Atmospheric Flight Mechanics Conference, Report AIAA-90-2836, *Bifurcation Analysis of a Model Fighter Aircraft with Control Augmentation*, Planeaux, J.B., Beck, J.A., Baumann, D.D., August 20-22, 1990.

6. Interview between Mr. Joseph Gera, Flight Controls Group Leader, NASA Ames Research Center/Dryden Flight Research Facility, and the author, 3 December 1990.

7. NAVAIR 01-F14AAA-1, *NATOPS FLIGHT MANUAL, NAVY MODEL F-14A AIRCRAFT*, 1 January 1986.

8. Grumman Aircraft Systems, Frederick W. Schaefer letter to LT. Steven R. Wright, subject: F14N7 CLEAN HIAOA DATABASE and Flight Time History Traces, 6 February 1991.

9. Grumman Aircraft Systems, Frederick W. Schaefer letter to Professor Louis Schmidt, subject: F14N7 CLEAN HIAOA DATABASE, 10 December 1990.

10. Etkin, B., *Dynamics of Flight-Stability and Control, Second Edition*, pp. 177-181 and 199-205, John Wiley & Sons, Inc., 1982.

11. McRuer, D., Ashkenas, I., Graham, D., *Aircraft Dynamics and Automatic Control*, pp. 292-295, Princeton University Press, 1973.

12. Ferziger, Joel H., *Numerical Methods for Engineering Application*, pp. 72-73, John Wiley & Sons, Inc., 1981.

13. *VF-126 Bandits Out of Control Flight Guide*, 89/405, pp. 17-18, FASO, 1989.

14. Ogata, K., *Modern Control Engineering*, Second Edition, pp. 722-725, Prentice-Hall, Inc., 1990.

BIBLIOGRAPHY

AIAA Atmospheric Flight Mechanics Conference, Report AIAA-80-1583, *Mathematical Modeling of the Aerodynamics of High-Angle-of-Attack Maneuvers*, Schiff, L.B., Tobak, M., Malcolm, G.N., August 11-13, 1980.

Nelson, R.C., *Flight Stability and Automatic Control*, McGraw-Hill, Inc., 1989.

Roskam, J., *Airplane Flight Dynamics and Automatic Flight Controls*, Roskam Aviation and Engineering Corporation, 1979.

INITIAL DISTRIBUTION LIST

1. Defense Technical Information Center — 2
   Cameron Station
   Alexandria, Virginia 22304-6145

2. Library, Code 52 — 2
   Naval Postgraduate School
   Monterey, California 93943-5100

3. Lt. Steven R. Wright — 3
   1216 Hickory Nut Dr.
   California, Maryland 20619

4. Dr. Louis V. Schmidt — 1
   Department of Aeronautics and Astronautics
   Code AA/Sc
   Naval Postgraduate School
   Monterey, California 93943-5000

5. Dr. Richard M. Howard — 1
   Department of Aeronautics and Astronautics
   Code AA/Ho
   Naval Postgraduate School
   Monterey, California 93943-5000

6. Dr. E. R. Wood — 1
   Chairman, Department of Aeronautics and Astronautics
   Code AA/Wd
   Naval Postgraduate School
   Monterey, California 93943-5000

7. Commander 1
Naval Air Systems Command
Attn: Code 530A
Washington, D.C. 20361

8. NASA/Ames Research Center 1
Dryden Flight Research Facility
Attn: Mr. Joseph Gera
P.O. Box 273
Edwards, California 93523

9. Grumman Aircraft Systems 1
Attn: Mr. Frederick W. Schaefer
Bethpage, New York 11714-3582